

Analysis and Optimization of Cache-Enabled mmWave HetNets with Integrated Access and Backhaul

Chenwu Zhang, Hancheng Lu, *Senior Member, IEEE*, and Zhuojia Gu

Abstract

In millimeter wave heterogeneous networks with [integrated access and backhaul](#) (mABHetNets), a considerable part of spectrum resources are occupied by the backhaul link, which limits the performance of the access link. In order to overcome such backhaul “*spectrum occupancy*”, we introduce cache in mABHetNets. Caching popular files at small base stations (SBSs) can offload the backhaul traffic and transfer spectrum from the backhaul link to the access link. To achieve the optimal performance of the cache-enabled mABHetNets, we first analyze the signal-to-interference-plus-noise ratio (SINR) distribution and derive the average potential throughput (APT) expression by stochastic geometric tools. Then, based on our analytical work, we formulate a joint optimization problem of cache decision and spectrum partition to maximize the APT. Inspired by the block coordinate descent (BCD) method, we propose a joint cache decision, spectrum partition and power allocation (JCSPA) algorithm to find the optimal solution. Simulation results show the convergence and enhancement of the proposed algorithm. Besides, we verify the APT under different parameters and find that the introduction of cache facilitates the transfer of backhaul spectrum to access link. [Jointly deploying appropriate caching capacity at SBSs and performing specified spectrum partition can bring up about 90% APT gain in mABHetNets.](#)

Index Terms

This work was supported in part by National Key R&D Program of China under Grant 2020YFA0711400 and National Science Foundation of China under Grant 61771445, 61631017, 91538203. [Part of this work has been presented at IEEE Wireless Communications and Networking Conference\(WCNC\), Seoul, South Korea, May, 2020 \[1\].](#)

Chenwu Zhang, Hancheng Lu and Zhuojia Gu are with CAS Key Laboratory of Wireless-Optical Communications, University of Science and Technology of China, Hefei 230027, China. (Email: cwzhang@mail.ustc.edu.cn; hclu@ustc.edu.cn; guzj@mail.ustc.edu.cn).

Millimeter wave, integrated access and backhaul (IAB), cache, spectrum transfer, average potential throughput (APT).

I. INTRODUCTION

The number of mobile terminal equipments increases sharply in recent years and the demand for data also increases at an annual growth rate of 63% [2], while the existing scarce LTE spectrum resources [3] severely affect the high-demand communication. Fortunately, owing to the characteristics of abundant spectrum in millimeter wave (mmWave), the high throughput communication has become possible by using mmWave in both the access and the backhaul link. However, mmWave signals are only suitable for short distance propagation and are blockage sensitive, so the base stations (BSs) need to be deployed densely in mmWave heterogeneous networks (HetNets), which in turn increases the backhaul traffic. Particularly, integrated access and backhaul (IAB) in mmWave HetNets (mABHetNets) has been standardized for the fifth generation (5G) mobile communication technology in the third generation partnership project (3GPP) Rel-16 [3]–[7]. In mABHetNets, macro base stations (MBSs) are connected to the mobile core network via high-speed fiber backhaul, but it is not practical to connect all small base stations (SBSs) to the mobile core network. High-power MBSs are overlaid by denser low-power mmWave SBSs where SBSs provide high rate service to the users by wireless access link and the MBS maintains the backhaul capacity of the SBSs by the wireless backhaul link.

Since the access and the backhaul links share the mmWave spectrum resources in mABHetNets, spectrum partition has a significant impact on the network performance and hence attracted many research attempts [13]–[16]. Authors in [13] proposed the resource partition strategies as the total spectrum is dynamically between access and backhaul, or a static partition is defined for the access and backhaul link to achieve the maximum coverage probability in mmWave HetNets. Authors in [14] explored the optimal partition of access and backhaul spectrum to maximize the rate coverage and authors in [15] leveraged allocated resource ratio between radio access and backhaul to study the maximization of network capacity by considering the fairness among SBSs. In [16], the beamforming and spectrum partition were jointly investigated to improve the network capacity of mABHetNets. Maria *et al.* in [17] optimized phase shift of Reconfigurable Intelligent Surface (RIS) element, bandwidth splitting among wireless access and backhaul, and transmission power to maximize the energy efficiency of RIS-aided IAB network.

However, even with optimal spectrum partition, a considerable part of mmWave spectrum resources are still occupied by the backhaul link to maintain the backhaul capacity. According to the findings in [14], up to 50% mmWave spectrum might be used in backhaul link to satisfy the high speed data traffic. Such a “*spectrum occupancy*” phenomenon of wireless backhaul link severely limits the transmission of wireless access link, which further affects the communication quality of users and degrades the spectrum resource utilization. Besides, several reports show that a few files with high popularity are often requested by users, and this increases the transmission pressure on the wireless backhaul link [18], [19]. Repeated transmission also causes a lot of waste of power consumption and spectrum resources. Fortunately, enabling caching at the wireless edge such as SBSs is considered as a promising way to improve the energy efficiency and network throughput recently [18]–[22], especially for those files with high popularity and frequently requested. In [19], Tao *et al.* proposed a cache-enabled radio access network (RAN) to minimize the total network cost. Authors in [20] applied coded caching into small-cell network (SCN) and investigated average fractional offloaded traffic (AFOT) and average ergodic rate (AER) performance metrics, then maximize the AFOT. In [21], Xu *et al.* proposed a cache-enabled HetNets with limited backhaul and analyzed the successful content delivery probability, successful delivery rate as well as energy efficiency theoretically. Caching those files proactively during off-peak time at the edge of the network can reduce the data traffic pressure of backhaul link [22]. When the backhaul traffic is offloaded by caching popular files at the cache of SBSs, a part of mmWave spectrum can be transferred from the backhaul link to the access link.

Although the introduction of cache brings the benefits of improvement the network throughput, nonetheless some new problems arise both theoretically and technically: how to deploy the cache appropriately to solve the “*spectrum occupancy*” problem, how much improvement the cache can bring to the throughput performance of the mABHetNets. Thus, it is essential to jointly consider the cache decision and spectrum partition in mABHetNets to improve the APT. In this paper, average potential throughput (APT) metric is used to measure the network performance, which has become the major performance metric in mmWave HetNets [9]–[12] and focuses on analyzing user’s average throughput with the specific rate requirement [9]. On the one hand, since each BS in cache-enabled mABHetNets has a limited energy resource and the energy consumed by additional cache can not be neglected [24], [26], caching capacity at SBS changes the signal-to-interference-plus-noise ratio (SINR) and coverage probability of user, which affects the corresponding spectrum partition strategy and further changes the allocation of resources(i.e.,

caching capacity, spectrum partition and power allocation) in mABHetNets. Therefore, in theory, APT in cache-enabled mABHetNets needs to consider the effect of the above factors. On the other hand, caching capacity as well as transmit power are limited by the maximum power constraint at SBS, which also affects the optimal spectrum partition coefficient and thus affect the APT, so these three resource variables are coupled with each other. To achieve desired APT in cache-enabled mABHetNets, the joint optimization algorithm needs to be further investigated. To address the aforementioned issues, in this paper, the main contributions are summarized as follows.

- We develop a tractable analytical framework from a stochastic geometry perspective and derive the user association probability via wireless access link as well as SBS association probability via wireless backhaul link based on the maximum biased received power, respectively. Considering the effect of blockage and directional beamforming, we derive the distance distribution between the different transmitters and receivers by taking the association probability into account. Then the APT expression is derived to measure the performance of cache-enabled mABHetNets. Under noise-limited scenario, a closed-form SINR distribution in APT expression can be obtained through stochastic geometry tools to provide some insights about our proposed cache-enabled mABHetNets.
- Based on our analytical work, an APT maximization problem is formulated where caching capacity, spectrum partition and power allocation are jointly considered; As the formulated problem is a mixed-integer nonlinear programming (MINLP) problem, we decompose it into two sub-problems, i.e., cache decision problem, spectrum partition and power allocation problem. Then, inspired by block coordinate descent (BCD) method, we propose a joint cache decision, spectrum partition and power allocation (JCSPA) algorithm to approach the optimal solution in an alternative manner;
- We investigate the effects of caching capacity and spectrum partition on APT both theoretically and experimentally. Some important insights on the interplay between caching capacity and spectrum partition are provided from the perspective of APT increment. Numerical simulation results are carried out to verify the convergence of proposed algorithm and show the effects of other cache-related parameters on APT. These indicate that joint optimization of cache decision and spectrum partition is an effective method to bring about 90% increment on APT beyond traditional mABHetNets.

The rest of the paper is organized as follows. Firstly, we introduce the system model of **cache-enabled** mABHetNets in Section II. Section III derives the SINR distribution of cache-enabled mABHetNets and then APT is further defined and derived based on the SINR distribution. Next, Section IV. gives the APT maximization problem and solution. Performance evaluation and numerical results are provided in Section V. Finally, the paper is concluded in Section VI.

II. SYSTEM MODEL

A. Network Model

In this section, we come up with a downlink cache-enabled mABHetNet with **integrated access and backhaul** architecture, which consists of an MBS tier and an SBS tier as shown in Fig. 1. In this architecture, high power MBSs are connected to core network via broad high rate optical fiber links and SBSs are associated with the corresponding MBS via providing mmWave spectrum wireless backhaul transmission links. **The typical user could be associated with both the MBS and SBS to obtain the wireless access service [27].** By stochastic geometry tool, the locations of the MBS and SBS are modeled as the independent Poisson Point Processes (PPPs), which are denoted by $\Phi_m \in \mathbb{R}_2$ and $\Phi_s \in \mathbb{R}_1$ with densities of λ_m and λ_s , respectively. We stipulate that the user density is large sufficiently so that each BS consists of at least one associated user in its coverage area. **We select a typical user at the origin for analysis. Based on Slivnyak's theorem in stochastic geometry, placing a point at the origin will not change the property of PPP.**

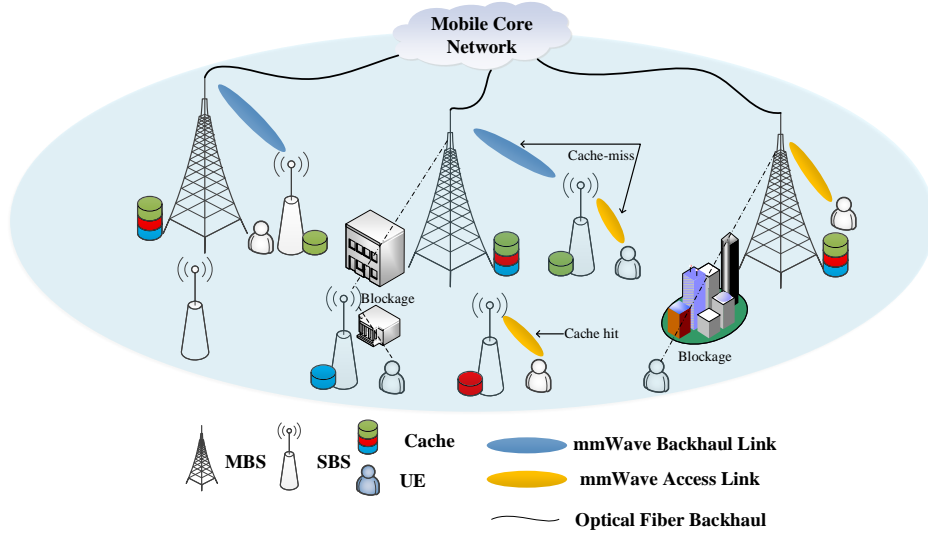


Fig. 1. An illustration of cache-enabled millimeter wave heterogeneous network with integrated access and backhaul.

B. Caching Model

The architecture we proposed in this paper is a cache-enabled HetNet. File library is denoted by symbol \mathcal{F} and the number of all files is $|\mathcal{F}| = F$. In order to derive conveniently, we assume that all the files in library have the same size and their size is expressed in file units. Such assumption can hold since those files can be divided into chunks of equal size in practical transmission [29]. In the whole file library, different files have different popularities and the popularity of the file often changes slowly or doesn't change in a short time [31]. The popularity of the file can be predicted according to interview records or machine learning retrieval methods and this research problem has been actively studied in recent years while it is outside the scope of this paper. In general, the popularity of the file obeys the Zipf distribution [24] [32]. For the files denoted by the index set $\mathcal{F} = [1, 2, \dots, f, \dots, F]$, the popularity of the file $f \in \mathcal{F}$ is $p_f = \frac{f^{-\gamma_p}}{\sum_{g=1}^F g^{-\gamma_p}}$, of which γ_p is the distribution parameter of the Zipf distribution and it denotes the skewness of Zipf distribution, while the bigger γ_p means that the fewer files have higher popularity [34]. In this paper, we use the highest-popularity-first cache strategy, which means that files with higher popularity will be cached preferentially. The caching capacity of MBS is large enough to load all the files in the file library [38], so the MBS caches all the F files. The partial files are deployed in the SBS according to the level of the popularity, so the SBS caches the C files in descending order of file popularity. From these we can also see that the MBS is 'Full-Cache' and the SBS is 'Partial-Cache'. Based on this, the cache hit ratio of the SBS is

$$p_h(C) = \frac{\sum_{f=1}^C f^{-\gamma_p}}{\sum_{g=1}^F g^{-\gamma_p}}. \quad (1)$$

C. Power Consumption Model

Like [23], the total power consumption model of the mABHetNet can be regarded as the power consumption of the MBS and SBS, where the power consumption of the MBS is $\rho_m P_m^{\text{tr}} + P_m^{\text{fc}} + P_m^{\text{ca}} = \rho_m P_m^{\text{tr}} + P_m^{\text{fc}} + \omega_{ca} s F$ and the power consumption of the SBS is $\rho_s P_s^{\text{tr}} + P_s^{\text{fc}} + P_s^{\text{ca}} = \rho_s P_s^{\text{tr}} + P_s^{\text{fc}} + \omega_{ca} s C$. ρ_m and ρ_s are the power consumption amplification factor of MBS and SBS transmitter. P_m^{fc} and P_s^{fc} are the fixed circuits-related power consumption of MBS and SBS [35]. P_m^{ca} and P_s^{ca} are the caching power consumption of MBS and SBS based on energy proportional model. In order to quantify the caching power consumption, widely used proportional power model [24], [25], [35]–[37] is introduced in this paper so that the caching power consumption is proportional to the cache file size such as $P_m^{\text{ca}} = \omega_{ca} s F$, $P_s^{\text{ca}} = \omega_{ca} s C$,

of which ω_{ca} is the coefficient of cache power consumption(unit:watt/bit). Assuming that the maximum power of each SBS has been preset, each SBS can adjust the transmit power and caching power(caching capacity) without exceeding the preset maximum power limit [25]. The actual transmit power consumption of the SBS and MBS are $P_s^{\text{tr}} = \frac{P_s^{\text{max}} - P_s^{\text{fc}} - \omega_{ca}sC}{\rho_s} = P'_s - \omega'_{ca}sC$, $P_m^{\text{tr}} = \frac{P_m^{\text{max}} - P_m^{\text{fc}} - \omega_{ca}sF}{\rho_m} = P'_m - \omega'_{ca}sF$, of which $P'_s = \frac{P_s^{\text{max}} - P_s^{\text{fc}}}{\rho_s}$, $\omega'_{ca}s = \frac{\omega_{ca}s}{\rho_s}$, $P'_m = \frac{P_m^{\text{max}} - P_m^{\text{fc}}}{\rho_m}$ and $\omega'_{ca} = \frac{\omega_{ca}s}{\rho_m}$. The relevant notations are summarized in the Table I.

TABLE I: Main Notations

Notation	Meaning	Notation	Meaning
$W/W_{ac}/W_{bh}$	Total spectrum/access link/backhaul link bandwidth	λ_m/λ_s	Density of MBS/SBS
α_L/α_{NL}	Path loss exponet of LOS/NLOS transmission	C	Caching capacity of SBS
η	mmWave bandwidth partition ratio for access link	C_{max}	Maximum caching capacity of SBS
$P_m^{\text{max}}/P_s^{\text{max}}$	Maximum power of MBS/SBS	F	Number of files in file library
$P_m^{\text{tr}}/P_s^{\text{tr}}$	Transmit power of MBS/SBS	p_h	Cache hit ratio of SBS
$P_m^{\text{fc}}/P_s^{\text{fc}}$	Fixed circuits-related power consumption of MBS/SBS	θ	Mainlobe beamwidth
$P_m^{\text{ca}}/P_s^{\text{ca}}$	Caching power consumption of MBS/SBS	B_m/B_s	The association bias factor of MBS/SBS
ρ_m/ρ_s	Power consumption amplification factor of MBS/SBS	s	Size of a file
M/m	The antenna gain of mainlobe/slide lobe	ω_{ca}	Caching power consumption coefficient

D. Channel and Transmission Model

In this paper, on account of the high density of MBS or SBS deployment and the linear propagation transmission characteristic of mmWave, each transmission link is assumed to be indepedent Nakagami-Rayleigh fading and the signals are based on the transmission link as either line-of-sight(LOS) or non-line-of-sight(NLOS). The path loss function expresses the signal attenuation relationship with distance r . The mathematical expression of the path loss function is as follows [39]:

$$L(r) = \begin{cases} A_L r^{-\alpha_L}, & \text{with LOS probability } \mathcal{P}_L(r), \\ A_{NL} r^{-\alpha_{NL}}, & \text{with NLOS probability } \mathcal{P}_{NL}(r) = 1 - \mathcal{P}_L(r), \end{cases} \quad (2)$$

of which the LOS probability $\mathcal{P}_L(r) = e^{-\beta r}$, $A_L(A_{NL})$ is the LOS(NLOS) pathloss parameter, r is the distance between the user and base station, $\alpha_L(\alpha_{NL})$ is a path loss exponent in LOS(NLOS) transmission of Nakagami fading. $\beta \geq 0$ is the parameter that captures density and size of obstacles between the transmitter and the reveicer. In practice, the probability of LOS transmission coverage is very close to one and NLOS transmission could be neglected.

Besides, directional beamforming are used for all antennas at the transceivers and signals propagates along the main lobe of the antenna. We use the sectorial antenna pattern in this analysis [40]. The antenna gain pattern for the transceiver in the mABHetNets is given as

$$G_q(\phi) = \begin{cases} M, & \text{if } |\phi| \leq \theta \\ m, & \text{otherwise.} \end{cases} \quad (3)$$

where $q \in \{T, R\}$ denotes the antenna at the transmitter or receiver, $\phi \in [0, 2\pi)$ is the angle off boresight direction, θ is the mainwidth of mainlobe, M and m are the gain of the main lobe and side lobe. Then the random gain for the transmission link and its probability is given as

$$G = \begin{cases} MM, & \text{with probability } \frac{\theta^2}{4\pi^2}, \\ Mm, & \text{with probability } \frac{\theta(2\pi - \theta)}{2\pi^2}, \\ mm, & \text{with probability } \frac{(2\pi - \theta)^2}{4\pi^2}. \end{cases} \quad (4)$$

For tractability of analysis, the perfect beamforming is assumed between the transmitter and receiver [41]. Based on the above analysis, we can derive the signal to interference plus noise ratio expression of a typical user from the associated SBS or the associated MBS via wireless access link at the distance r as follows.

$$\text{SINR}_s(r_s) = \frac{P_s^{tr} B_s G_s h_s L(r_s)}{I_s + I_m + N_0} = \frac{(P'_s - \omega'_{ca} C) B_s G_s h_s L(r_s)}{\sum_{i \in \Phi_s \setminus b_{s,0}} (P'_s - \omega'_{ca} C) B_s G_i h_{s,i} L(r_{s,i}) + \sum_{l \in \Phi_m} P_m^{tr} B_m G_l h_{m,l} L(r_{m,l}) + N_0}, \quad (5)$$

$$\text{SINR}_m(r_m) = \frac{P_m^{tr} B_m G_m h_m L(r_m)}{I'_s + I'_m + N_0} = \frac{(P'_m - \omega'_{ca} F) B_m G_m h_m L(r_m)}{\sum_{i \in \Phi_s} (P'_s - \omega'_{ca} C) B_s G_i h_{s,i} L(r_{s,i}) + \sum_{l \in \Phi_m \setminus b_{m,0}} P_m^{tr} B_m G_l h_{m,l} L(r_{m,l}) + N_0}, \quad (6)$$

where $b_{s,0}$ and $b_{m,0}$ denotes the serving SBS and MBS for user, B_s and B_m are the association bias factor of SBS and MBS, G_m , G_s , G_i and G_l are the antenna gain of the corresponding transmission link ($G_m = G_s = MM$). $h_{s,i}$ and $h_{m,l}$ are the small-scale fading from i -th SBS or j -th SBS ($h_s = h_m \sim \exp(1)$). $L(r_s)$ $L(r_m)$ are the path loss from the serving SBS or MBS to the typical user. r_s is the distance between the association SBS $b_{s,0}$ and the typical user. r_m is the distance between the association MBS $b_{m,0}$ and the typical user. $L(r_{s,i})$ is path loss from the i -th SBS to the typical user. $L(r_{m,l})$ is the path loss from the l -th MBS to the typical user. N_0 is the additive white Gaussian noise component. Besides, the MBS provides the wireless backhaul link to the SBS for data transmission. Similar to (5) and (6), for a typical SBS at a random

distance r_{bh} from its associated MBS, the SINR of the signal from the MBS to the SBS of the downlink backhaul link is then given as follows.

$$\text{SINR}_{bh}(r_{bh}) = \frac{P_m^{tr} B_m \mathbf{G}_m h_m L(r_{bh})}{I_{bh} + N_0} = \frac{(P'_m - \omega_{ca}'^m F) B_m \mathbf{G}_m h_m L(r_{bh})}{\sum_{i \in \Phi_m \setminus b_{m,0}} P_m^{tr} B_m \mathbf{G}_i h_{m,i} L(r_{bh,i}) + N_0}. \quad (7)$$

The symbol have similar meanings with (5) and (6).

E. Spectrum Partition Strategy

In this section, we will introduce the spectrum partition strategies in the downlink mABHetNet. W is the whole millimeter wave spectrum bandwidth available for the mABHetNet. To avoid the spectrum interference, the spectrum of access and backhaul link is orthogonal, so the whole spectrum needs to be divided into two parts: W_{bh} for the backhaul link and W_{ac} for the access link. Then we will introduce two bandwidth allocation strategies in the following.

1) *Fixed Spectrum Allocation(FSA)*: This default spectrum allocation strategy is widely used in traditional heterogeneous network. In order to satisfy the communication needs fairly, we allocate spectrum for the access and backhaul link equally as $W_{bh} = 0.5W$ and $W_{ac} = 0.5W$ (W is the total spectrum bandwidth). In this case, we will give the transmission data rate based on Shannon's theorem of backhaul link and access link, respectively.

$$R_i = \frac{1}{2} W \log_2(1 + \text{SINR}_i), \quad (8)$$

where $i = \{bh, m, s\}$ denotes the backhaul link, MBS tier or SBS tier via access link.

2) *Dynamic Spectrum Allocation(DSA)*: In order to alleviate “*spectrum occupancy*” problem, we introduce a parameter η to allocate spectrum dynamically according to the current caching status at SBS, where $\eta \in [0, 1]$ is the spectrum partition ratio coefficient for the access link so the spectrum for the backhaul link is $W_{bh} = (1 - \eta)W$ and the spectrum for the access link is $W_{ac} = \eta W$. Users are usually accessed to the SBSs and file delivery needs to go through the backhaul link, so the access link is cache-miss when the files requested at not cached at the SBS. In other words, the file delivery rate depends on both the access link rate and the backhaul link rate. Similarly, we give the transmission data rate of each link as follows.

$$R_{bh} = (1 - \eta) W \log_2(1 + \text{SINR}_{bh}), \quad (9)$$

$$R_s = \eta W \log_2(1 + \text{SINR}_s), \quad (10)$$

$$R_m = \eta W \log_2(1 + \text{SINR}_m). \quad (11)$$

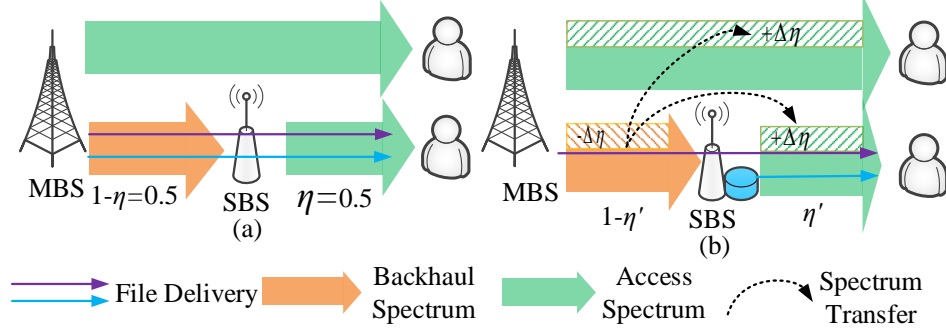


Fig. 2. Spectrum partition strategies between access and backhaul link, (a) Fixed Spectrum Allocation(FSA), (b) Dynamic Spectrum Allocation(DSA).

III. SINR DISTRIBUTION AND APT ANALYSIS OF MABHETNET

In this section, we will derive the expression of SINR distribution of the typical user conditioned on its association selections. As users are covered by the associated SBS, we first derive the PDF of the distance between the user and the serving SBS. Further, SINR distributions of the SBS associated with the serving MBS are also obtained. Finally, we derive the APT expression of cache-enabled mABHetNets.

A. The PDF of Distance to Nearest Base Station

First of all, we need to derive the probability distribution function (PDF) of the distance between the typical user and its nearest SBS. We focus on the typical user at the origin. When the typical user communicates with the closest SBS at a distance r , no other SBS can be closer than r . Since the typical user is associated with the closest SBS via either LOS or NLOS channel, we derive these PDFs in the following Lemma.

Lemma 1. *The PDF of r (the distance between the typical user and the nearest SBS via a LOS/NLOS path) is written as*

$$f_{R_s}^k(r) = \mathcal{P}_k(r) \times \exp(-\pi r^2 \lambda_s) \times 2\pi r \lambda_s, \quad (12)$$

where s denotes the index of SBS tier, $k = \{L, NL\}$ denotes the transmission path of LOS or NLOS in wireless access link.

Proof. The proof process is provided in Appendix VII-A. □

Remark 1. Similarly to Lemma 1, the uncached file data will be delivered from the MBS to the SBS by the wireless backhaul link of mmWave. Similar to the above analysis in Lemma 1, the PDF of distance r (between the SBS and the associated the nearest MBS via a LOS/NLOS path) can be written as

$$f_{R_{bh}}^k(r) = \mathcal{P}_k(r) \times \exp(-\pi r^2 \lambda_m) \times 2\pi r \lambda_m, \quad (13)$$

where bh denotes the index of backhaul link and k is the same as (12).

B. Association Probability

In the mABHetNet, we will first analyze the probability that a user is associated with SBS tier via different path due to the different transmission path and the densities of the SBS and MBS. Besides, since SBS may be associated with MBS via different transmission paths in the SBS backhaul association, different SBS backhaul association probabilities should be derived in the meanwhile.

1) *user association probability:* We consider a user association based on maximum biased received power, where a mobile user is associated with the strongest SBS in terms of the received power at the user. Then, for a typical user associated with the SBS tier via LOS path and NLOS path, the received powers are $P_s^{tr} B_s G_s h_s A_L r^{-\alpha_L}$ and $P_s^{tr} B_s G_s h_s A_{NL} r^{-\alpha_{NL}}$, respectively. Based on the maximum biased received power association strategy, the BS density and transmit power as well as transmission path determine the probability that a typical user is associated with an SBS. The following lemma provides the SBS association probability via LOS and NLOS path respectively.

Lemma 2. For the given distance r , the probabilities that a typical user is associated with the SBS tier by LOS link and NLOS link are

$$F_s^L(r) = p_{ln}^{ss}(r) p_{ll}^{sm}(r) p_{ln}^{sm}(r) f_{R_s}^L(r), \quad (14)$$

$$F_s^{NL}(r) = p_{nl}^{ss}(r) p_{nl}^{sm}(r) p_{nn}^{sm}(r) f_{R_s}^{NL}(r), \quad (15)$$

Then, the probabilities that a typical user is associated with the MBS tier by LoS link and NLoS link are

$$F_m^L(r) = p_{ln}^{mm}(r) p_{ll}^{ms}(r) p_{ln}^{ms}(r) f_{R_m}^L(r), \quad (16)$$

$$F_m^{NL}(r) = p_{nl}^{mm}(r) p_{nl}^{ms}(r) p_{nn}^{ms}(r) f_{R_m}^{NL}(r) \quad (17)$$

where $p_{ln}^{ss}(r) = e^{-\lambda_s \pi \left[\left(\frac{A_L}{A_{NL}} \right)^{\frac{-1}{\alpha_{NL}}} r^{\frac{\alpha_L}{\alpha_{NL}}} \right]^2}$ denotes the probability of the event that the user obtains the desired LOS signal from SBS and the NLOS interference from the SBS. Other notations have similar definition and can be found in the proof.

Proof. The proof process is provided in Appendix VII-B. \square

2) *SBS backhaul association probability:* The SBS will be associated with the MBS by the wireless backhaul link. The SBS backhaul association strategy is also based on the maximum biased received power from the MBS. Since the backhaul transmission includes LOS link and NLOS link, there exist two backhaul association probabilities. These probabilities are given in the following remark.

Remark 2. Similar to Lemma 2, the probabilities that a typical SBS is associated with the MBS tier by LOS link and NLOS link are

$$F_{bh}^L(r) = p_{ln}^{bh}(r) f_{R_{bh}}^L(r), \quad (18)$$

$$F_{bh}^{NL}(r) = p_{nl}^{bh}(r) f_{R_{bh}}^{NL}(r), \quad (19)$$

where $p_{ln}^{bh}(r) = e^{-\lambda_m \pi \left[\left(\frac{A_L}{A_{NL}} \right)^{\frac{-1}{\alpha_{NL}}} r^{\frac{\alpha_L}{\alpha_{NL}}} \right]^2}$ is the probability that the SBS is associated with the MBS in LOS link and the interference is from MBS in NLOS link. $p_{nl}^{bh}(r)$ has the similar definition.

C. SINR Distribution

To study the APT performance of mABHetNet, we need to first investigate the SINR distribution of the user covered by SBS tier via access link and the SINR distribution of the SBS covered by MBS via backhaul link. This SINR distribution is defined as the probability that the received SINR is above a pre-designated threshold γ :

$$P^{\text{cov}}(\gamma) = \Pr[\text{SINR} > \gamma]. \quad (20)$$

Since the user is covered by SBS, we first give the SINR distribution of the user. Then we give the SINR distribution of the typical SBS which is covered by MBS.

Proposition 1. 1) *SINR distribution of user covered by the SBS or the MBS :*

The SINR distribution that the typical user is associated with the SBS via access link is:

$$\mathbb{P}_s^{\text{cov}}(\gamma) = \sum_{i=L, NL} P_{s,i}^{\text{cov}}(\gamma), \quad (21)$$

$$P_{s,i}^{cov}(\gamma) = \int_0^\infty \exp\left(\frac{-\gamma N_0}{P_s^{tr} B_s \mathbf{G}_s A_i r^{-\alpha_i}}\right) \mathcal{L}_{I_{s,m}}^i F_s^i(r) dr, \quad (22)$$

of which s denotes the SBS, $i = \{L, NL\}$ denotes the transmission link. $\mathbf{G}_s = MM$, $P_{s,i}^{cov}(\gamma) = \mathbb{E}_r [\mathbb{P} [\text{SINR}_s^i(r) \geq \gamma]]$ is the probability that the user is covered by the SBS, where s denotes SBS, γ is the default threshold for successful demodulation and decoding at the receiver and the Laplace transform of interference from SBS or MBS in LOS link is given as

$$\begin{aligned} \mathcal{L}_{I_{s,m}}^L(\gamma r^{\alpha_L}) &\stackrel{(b)}{=} \prod_{G_i} \exp\left(-2\pi\lambda_s p_{G_i} \left(\int_r^\infty \frac{\mathcal{P}_L(u)u}{1 + \frac{P_s^{tr} B_s \mathbf{G}_s A_L r^{-\alpha_L}}{\gamma P_s^{tr} B_s \mathbf{G}_i A_L u^{-\alpha_L}}} du + \int_{\left(\frac{A_L}{A_{NL}}\right)^{\frac{-1}{\alpha_{NL}}}} \frac{\mathcal{P}_{NL}(u)u}{1 + \frac{P_s^{tr} B_s \mathbf{G}_s A_L r^{-\alpha_L}}{\gamma P_s^{tr} B_s \mathbf{G}_i A_{NL} u^{-\alpha_{NL}}}} du\right)\right) \\ &\quad \times \prod_{G_l} \exp\left(-2\pi\lambda_m p_{G_l} \left(\int_{(d_1)^{\frac{-1}{\alpha_L}}} \frac{\mathcal{P}_L(u)u}{1 + \frac{P_s^{tr} B_s \mathbf{G}_s A_L r^{-\alpha_L}}{\gamma P_m^{tr} B_m \mathbf{G}_l A_L u^{-\alpha_L}}} du + \int_{(d_2)^{\frac{-1}{\alpha_{NL}}}} \frac{\mathcal{P}_{NL}(u)u}{1 + \frac{P_s^{tr} B_s \mathbf{G}_s A_L r^{-\alpha_L}}{\gamma P_m^{tr} B_m \mathbf{G}_l A_{NL} u^{-\alpha_{NL}}}} du\right)\right), \end{aligned}$$

where $G_i, G_l \in \{MM, Mm, mm\}$, $p_{G_i}(p_{G_l})$ is the probability of the antenna gain taking corresponding value from SBS interference tier and MBS interference tier. $d_1 = \frac{P_s^{tr} B_s}{P_m^{tr} B_m}$ and $d_2 = \frac{P_s^{tr} B_s A_L}{P_m^{tr} B_m A_{NL}}$. Following the same logic, other Laplace transform of interference have similar expressions.

Remark 3. From the Laplace transform of interference, the interference from the SBS tier is independent of the transmit power P_s^{tr} and even the interference from the MBS layer is monotonically decreasing about P_s^{tr} , which also reveals that increasing the transmit power P_s^{tr} is beneficial to improve the coverage probability and APT without considering other constraints. Such proof precess can be done by substituting the interference term into the Laplace transform.

Similarly, the SINR coverage probability that the user is associated with the MBS is

$$\mathbb{P}_m^{cov}(\gamma) = \sum_{i=L, NL} P_{m,i}^{cov}(\gamma), \quad (23)$$

$$P_{m,i}^{cov}(\gamma) = \int_0^\infty \exp\left(\frac{-\gamma N_0}{P_m^{tr} B_m \mathbf{G}_m A_i r^{-\alpha_i}}\right) \mathcal{L}_{I_{s,m}}^i(\gamma r^{\alpha_i}) F_m^i(r) dr \quad (24)$$

2) SINR distribution of SBS covered by MBS:

The SINR distribution that the typical SBS is covered by the MBS via backhaul link is:

$$\mathbb{P}_{bh}^{cov}(\gamma) = \sum_{i=L, NL} P_{bh,i}^{cov}(\gamma), \quad (25)$$

$$P_{bh,i}^{cov}(\gamma) = \int_0^\infty \exp\left(\frac{-\gamma N_0}{P_m^{tr} B_m \mathbf{G}_m A_i r^{-\alpha_i}}\right) \mathcal{L}_{I_{bh}}^i(\gamma r^{-\alpha_i}) F_{bh}^i(r) dr, \quad (26)$$

where the subscript *bh* denotes the backhaul, *i* also represents the transmission link and $G_m = MM$. Note that, considering a more general fading model such as Nakagami does not provide any additional design insights, but it does complicate the analysis significantly. Similar to [42] in our paper, the special case of Rayleigh fading is considered.

Proof. The proof process is provided in Appendix VII-C. \square

Proposition 2. In noise-limited scenario ($\sigma^2 \gg I$), the SINR distribution can be reduced into a closed-form as

$$P_k^{cov}(\gamma) = 1 - \exp \left(-\pi \lambda_k A_{NL}^{\frac{2}{\alpha_{NL}}} \Gamma \left(\frac{1}{\alpha_{NL}} + 1 \right) \left(\frac{P_k B_k G_k}{\sigma^2 \gamma} \right)^{\frac{2}{\alpha_{NL}}} - 2\pi \lambda_k Y \left(\frac{P_k B_k G_k}{\sigma^2 \gamma} \right) \right), \quad (27)$$

where $Y(\xi_0) = \int_0^{\xi_0} \frac{A_L^{\frac{2}{\alpha_L}-1}}{\alpha_L \xi^2} \int_0^\infty \phi^{\frac{2}{\alpha_L}} \exp(-\beta \phi^{\frac{1}{\alpha_L}} - \frac{\phi}{\xi}) d\phi d\xi - \int_0^{\xi_0} \frac{A_{NL}^{\frac{2}{\alpha_{NL}}-1}}{\alpha_{NL} \xi^2} \int_0^\infty \phi^{\frac{2}{\alpha_{NL}}} \exp(-\beta \phi^{\frac{1}{\alpha_{NL}}} - \frac{\phi}{\xi}) d\phi d\xi$, $k \in \{m, s\}$ denotes the MBS tier or the SBS tier.

Proof. The detailed proof process of Proposition2 is provided in the Appendix. \square

D. APT of Cache-enable mABHetNet

APT is a significant metric to measure the heterogeneous network performance, which mainly focuses on the average user QoS requirement in terms of data rate. Next, we will derive the APT expressions based on the above analysis.

1) *Definition:* APT captures the average number of bits that can be received by user per unit area per unit bandwidth for a given pre-designated threshold γ_0 [9]. The definition of APT is

$$\mathcal{R}(\gamma_0) = \lambda_k W \log_2(1 + \gamma) \mathbb{P}\{\text{SINR} \geq \gamma_0\}, \quad (28)$$

where $\lambda_k, k \in \{m, s\}$ is the density of MBS or SBS and W is the allocated spectrum. γ_0 is SINR threshold for the signal demodulation and represents the receiver's communication requirement.

2) *The detailed APT expression:* APT of mABHetNet depends on both the backhaul link and the access link, then we will give the detailed expression in the following analysis.

For the user associated with the SBS, the transmission link includes the backhaul link between the MBS and SBS and the access link between the SBS and user. Besides, in this cache-enabled mABHetNet, the cache in SBS also influence the file delivery in the transmission path. When

the requested files are cached at the SBS, the files can be delivered to user directly without transmitting through the wireless backhaul link. In other words, the wireless backhaul link will not be occupied under cache-hit circumstance. Besides, if the files requested by user are not cached at the SBS, the missing files need to be delivered from the MBS, which increases the wireless backhaul traffic. In this case, the user's APT depends on the minimum throughput of the backhaul link and the access link. *For the user associated with MBS, APT depends on the access link.* Given that the partial files are cached in SBS, we give the APT expression of mABHetNet in the following corollary.

Corollary 1. *Since the transmission can be LOS or NLOS in wireless access and backhaul link for user associated with SBS tier or MBS tier, we can get the APT of SBS tier, MBS tier and mABHetNet respectively. First, we give the APT expression of SBS tier.*

$$\mathcal{R}_s(\eta, C, P_s^{\text{tr}}) = \min\{(1 - p_h(C))\lambda_s\eta W \log_2(1 + \gamma_0)P_s^{\text{cov}}(P_s^{\text{tr}}), \\ (1 - p_h(C))\lambda_m W(1 - \eta) \log_2(1 + \gamma_0)P_{bh}^{\text{cov}}(P_m^{\text{tr}})\} + p_h(C)\lambda_s\eta W \log_2(1 + \gamma_0)P_s^{\text{cov}}(P_s^{\text{tr}}), \quad (29)$$

where $P_s^{\text{cov}}(P_s^{\text{tr}}) = \sum_{i=L,NL} P_{s,i}^{\text{cov}}(P_s^{\text{tr}})$, $P_{bh}^{\text{cov}}(P_m^{\text{tr}}) = \sum_{i=L,NL} P_{bh,i}^{\text{cov}}(P_m^{\text{tr}})$ denotes the SINR coverage probability of wireless access link for user associated with SBS tier, wireless backhaul link for SBS associated with MBS, respectively. The Symbol $\min\{\}$ means that the minimum value of throughput in the wireless access link of SBS tier and throughput in the wireless backhaul link. The APT of MBS tier is given as follows.

$$\mathcal{R}_m(\eta) = \lambda_m\eta W \log_2(1 + \gamma_0)P_m^{\text{cov}}(P_m^{\text{tr}}) \quad (30)$$

where $P_m^{\text{cov}}(P_m^{\text{tr}}) = \sum_{i=L,NL} P_{m,i}^{\text{cov}}(P_m^{\text{tr}})$ is the SINR coverage probability of wireless access link for user associated with MBS tier. Then, APT of mABHetNets can be obtained as follows.

$$\mathcal{R}(\eta, C, P_s^{\text{tr}}) = \mathcal{R}_s(\eta, C, P_s^{\text{tr}}) + \mathcal{R}_m(\eta) \quad (31)$$

Note that, C is the caching capacity of SBS and $p_h = p_h(C) = \frac{\sum_{f=1}^C f^{-\gamma_p}}{\sum_{g=1}^F g^{-\gamma_p}}$ is the cache hit ratio in the SBS tier. $(1 - p_h)$ reflects the probability that the files are not cached in SBS tier and need to be delivered through the backhaul link. $P_{s,L}^{\text{cov}}$ and $P_{k,NL}^{\text{cov}}, k \in \{s, m, bh\}$ is the SINR distribution of wireless LOS link and NLOS link in Proposition 1.

IV. PROBLEM FORMULATION AND SOLUTION

In this section, we propose an APT maximization problem with multivariate function and complicated integral component. Inspired by BCD method, we propose a two-step approach

to solve it alternately and decompose the joint optimization problem into two sub-problems to obtain the optimal spectrum partition coefficient, power allocation as well as cache decision, respectively. Therefore, we can solve these two small-scale sub-problems iteratively.

A. APT maximization problem

Based on the above theoretical analysis with stochastic geometry, in order to further explore the potential performance superiority of the cache-enabled mABHetNets, we formulate a joint optimization problem of cache, transmit power and spectrum partition to maximize the APT.

$$\mathcal{P} : \max_{C, \eta, P_s^{\text{tr}}} \min \{ (1 - p_h) \lambda_m (1 - \eta) W \log_2(1 + \gamma_0) P_{bh}^{\text{cov}}(P_m^{\text{tr}}), (1 - p_h) \lambda_s \eta W \log_2(1 + \gamma_0) P_s^{\text{cov}}(P_s^{\text{tr}}) \} \\ + p_h \lambda_s \eta W \log_2(1 + \gamma_0) P_s^{\text{cov}}(P_s^{\text{tr}}) + \lambda_m \eta W \log_2(1 + \gamma_0) P_m^{\text{cov}}(P_m^{\text{tr}}) \quad (32a)$$

$$s.t. \rho_s P_s^{\text{tr}} + P_s^{\text{fc}} + \omega_{\text{ca}} s C \leq P_s^{\text{max}}, \quad (32b)$$

$$P_s^{\text{tr}} \geq 0, \quad (32c)$$

$$C \in \{0, 1, 2, \dots, C_{\text{max}}\}, \quad (32d)$$

$$\eta \in [0, 1]. \quad (32e)$$

Constraint (32b) guarantees that the power consumed by the SBS will not exceed the maximum power constraint P_s^{max} . Constraint (32c) ensures that the transmitted power is non-negative. Constraint (32d) denotes that the number of the files cached at the SBS is a discrete variable from 0 to C_{max} , where C_{max} is the maximum caching capacity (file units) of the SBS. Constraint (32e) determines that spectrum partition coefficient is a continuous variable from 0 to 1.

From the above expression, we can easily get that the proposed problem P is a max-min and a mixed-integer nonlinear programming (MINLP) problem, which is non-linear and non-convex. To simplify the problem and facilitate the solution, we introduce an auxiliary variable Y to convert the problem P into a more tractable form as $\mathcal{P}1$.

$$\mathcal{P}1 : \max_{C, \eta, P_s^{\text{tr}}} Y \quad (33a)$$

$$s.t. (1 - p_h) \lambda_m (1 - \eta) W \log_2(1 + \gamma_0) P_{bh}^{\text{cov}}(P_m^{\text{tr}}) + p_h \lambda_s \eta W \log_2(1 + \gamma_0) P_s^{\text{cov}}(P_s^{\text{tr}}) + \lambda_m \eta W \log_2(1 + \gamma_0) P_m^{\text{cov}}(P_m^{\text{tr}}) \geq Y, \quad (33b)$$

$$(1 - p_h) \lambda_s \eta W \log_2(1 + \gamma_0) P_s^{\text{cov}}(P_s^{\text{tr}}) + p_h \lambda_s \eta W \log_2(1 + \gamma_0) P_s^{\text{cov}}(P_s^{\text{tr}}) + \lambda_m \eta W \log_2(1 + \gamma_0) P_m^{\text{cov}}(P_m^{\text{tr}}) \geq Y, \quad (33c)$$

$$(32b), (32c), (32d), (32e).$$

Proposition 3. *APT in cache-enabled millimeter wave HetNets will be maximized when the SBS consumes the maximum power, i.e., satisfy*

$$\rho_s P_s^{\text{tr}} + P_s^{\text{fc}} + \omega_{\text{ca}} s C = P_s^{\text{max}}. \quad (34)$$

Proof. When the power consumption satisfies $\rho_s P_s^{\text{tr}} + P_s^{\text{fc}} + \omega_{\text{ca}} s C < P_s^{\text{max}}$, the SBS can increase its caching power to $P_s^{\text{max}} - \rho_s P_s^{\text{tr}} - P_s^{\text{fc}}$ for a higher cache hit ratio, so introducing the caching without reducing the transmit power can increase the APT. Based on proof by contradiction, we can get that the SBS consumes the maximum power when APT is maximized. Thus transmit power at the SBS can be denoted as $P_s^{\text{tr}} = P'_s - \omega'_{\text{ca}} s C$ \square

Remark 4. *From the above analysis, increasing the caching capacity leads to the spectrum transfer and increasing the APT. However, from constraint (32b), we can see that APT is not a monotonically increasing function of C . Transmit power and caching capacity are coupled variables. This reveals that increasing the caching capacity is adverse to improving the APT when APT is limited by the transmit power.*

B. Sub-problem: Spectrum Partition Problem

In this subsection, we will give the solution of the spectrum partition problem when the cache decision and transmit power is given. To simplify the notation, we stipulate that $A_1 = \lambda_m W \log_2(1 + \gamma_0)$, $A_2 = \lambda_s W \log_2(1 + \gamma_0)$, $A_3 = \lambda_m W \log_2(1 + \gamma_0)$. Then the original problem can be transformed to the spectrum partition problem as $\mathcal{P}2$.

$$\mathcal{P}2 : \max_{Y, \eta} Y \quad (35a)$$

$$s.t. A_1(1 - p_h)(1 - \eta)P_{bh}^{\text{cov}} + A_2 p_h P_s^{\text{cov}} \eta + A_3 \eta P_m^{\text{cov}} \geq Y, \quad (35b)$$

$$A_2 \eta P_s^{\text{cov}} + A_3 \eta P_m^{\text{cov}} \geq Y, \quad (35c)$$

$$(32b), (32c), (32d), (32e).$$

of which $P_k^{\text{cov}}, k = \{s, m, bh\}$ is an integral term containing the transmit power of the SBS or MBS. It's obvious that this sub-problem becomes a linear constraint programming problem of variable Y and η , of which Y is the corresponding APT and η is the solution of spectrum partition coefficient. We can solve this problem by interior point method to get the η^* and the corresponding Y^* directly. The spectrum partition problem is based on interior-point method to obtain the optimal spectrum partition coefficient (one variable) with complexity $\mathcal{O}(1)$.

C. Sub-problem: Cache Decision and Power Allocation Problem

In this subsection, we will optimize the cache decision C and power allocation P_s^{tr} problem based on the given spectrum partition coefficient η , which is still a discrete, nonlinear and non-convex optimization problem. Based on an genetic algorithm, we propose a genetic-based cache decision and power allocation algorithm which is elaborated in Algorithm 1 to give the approximate optimal solution in feasible time. Therefore, the cache decision and power allocation problem is reformulated as $\mathcal{P}3$.

$$\mathcal{P}3 : \max_{Y, C, P_s^{tr}} Y \quad (36a)$$

$$s.t. A_1(1 - p_h)(1 - \eta)P_{bh}^{\text{cov}} + A_2p_h\eta P_s^{\text{cov}}(P_s^{tr}) + A_3\eta P_m^{\text{cov}} \geq Y, \quad (36b)$$

$$A_2\eta P_s^{\text{cov}}(P_s^{tr}) + A_3\eta P_m^{\text{cov}} \geq Y, \quad (36c)$$

$$(32b), (32c), (32d), (32e).$$

In order to simplify the problem even further and from Proposition 3, we stipulate that $f_1(C) = A_1(1 - p_h(C))(1 - \eta)P_{bh}^{\text{cov}} + A_2p_h(C)\eta P_s^{\text{cov}}(P'_s - \omega'_{ca}C) + A_3\eta P_m^{\text{cov}}$, $f_2(C) = A_2\eta P_s^{\text{cov}}(P'_s - \omega'_{ca}C) + A_3\eta P_m^{\text{cov}}$, then we optimize the minimum value of these two constraint functions according to an Genetic-based Cache Decision and Power Allocation (GCDPA) algorithm. This algorithm is based on heuristic algorithm to make cache decision designed for SBS. The worst case for cache decision algorithm at each SBS is to traverse all feasible solutions with complexity $\mathcal{O}(C_{\max})$.

D. Joint optimization solution

In view of the fact that this joint optimization problem is a non-convex and multivariate problem, we propose an alternating optimization algorithm to optimize spectrum partition and cache decision, which is described in Algorithm 2. The idea of iterative optimization is inspired by the BCD method proposed in [51]. BCD is a method for optimizing multivariate function even if it is neither necessarily strictly convex nor differentiable [52]. In each iteration, it takes the extremum along the direction of multiple coordinate axes (variables), and one of the coordinates or the coordinate blocks is fixed to optimize another coordinate or coordinate block, then the new result is immediately substituted into the next iteration. Particularly, the block coordinate iteration method will converge in a finite number of times as long as the two variables have no strong correlation. The JCSPA algorithm is based on BCD method to optimize subproblem of spectrum partition and subproblem of cache decision and power allocation alternately, so the

Algorithm 1: Genetic-based Cache Decision and Power Allocation Algorithm(GCDPA)

Input: Initial $\mathcal{C} = \mathcal{C}_1$; Spectrum partition ratio η from first sub-problem;

Generation size: \mathcal{S}^g ; Chromosome size: \mathcal{S}^c ; Population size: \mathcal{S}^p ; Crossover rate: ρ_c ;

Mutation rate: ρ_m ; Fitness functions $f(\mathcal{C}) = \min\{f_1(\mathcal{C}), f_2(\mathcal{C})\}$;

Output: Best individual \mathcal{C}^* ; Best fitness value $f^*(\mathcal{C})$;

```

1 Optimize fitness function;
2  $\mathcal{C}^1 = \text{Initialization}(\mathcal{S}^c, \mathcal{S}^p)$ ;
3 for  $k = 1; k < \mathcal{S}^g; k++$  do
4    $\mathcal{C}^*, f^*(\mathcal{C}) = \text{Fitness Function}(\mathcal{C}^k)$ ;
5    $\mathcal{C}^k = \text{Selection}(\mathcal{C}^k, f^*(\mathcal{C}))$ ;
6    $\mathcal{C}^k = \text{Crossover}(\mathcal{C}^k, \rho_c)$ ;
7    $\mathcal{C}^k = \text{Mutation}(\mathcal{C}^k, \rho_m)$ ;
8   Return  $\mathcal{C}^*, f^*(\mathcal{C})$ ;
9 end
10 Output  $\mathcal{C}^*, f^*(\mathcal{C})$ ;

```

worst case is to iterate to the maximum iteration times $Iter_{\max}$. The complexity of entire JCSPA algorithm is upper bound by $\mathcal{O}(C_{\max} * Iter_{\max})$. We further illustrate the optimality of Algorithm 2 in the following theorem.

Theorem 1. *Algorithm 2 based on BCD method will converge in finite number of iterations and the convergent output η^*, C^* is the [approach](#) to the optimal solution of the original problem P .*

This theorem can be proved that these two sub-problems have a unique optimal solution. Then based on basic cyclic rule, the consequences from BCD method is defined and bounded and the constraint set is a Cartesian product of closed convex sets. In proposed JCSPA algorithm, after Proposition 3, the spectrum partition coefficient η and caching decision C are optimized in turn while keeping the other fixed, with the goal of maximizing APT. After spectrum partition solution for fixed C_t , it will hold that

$$APT(\eta_t, C_t) \leq APT(\eta_{t+1}, C_t) \quad (37)$$

Algorithm 2: Joint Cache Decision, Spectrum Partition and Power Allocation Alternative Optimization Algorithm(JCSPA)

Input: Parameter of simulation scenario; Maximum number of iterations $Itermax$; ϵ

Output: Optimal cache decision \mathcal{C}^* and spectrum partition η^* .

```

1 Initial procedure:
2 Set  $t = 0$ ;
3 Strating point  $\mathcal{C}^{(0)}$ ;
4  $APT_1^{(0)} = 0, APT_2^{(0)} = 0$ ;
5 end Initial procedure;
6 repeat
7   Set  $t = t + 1$ ;
8   Update  $\eta^{(t)}$  for fixed  $\mathcal{C}^{(t-1)}$  according to (35a) and send it to next sub-problem, then
     calculate the corresponding  $APT_1^{(t)}$  according to (32a);
9   Solve sub-problem of cache decision for given  $\eta^{(t)}$  based on Algorithm 1 to get  $\mathcal{C}^{(t)}$ ,
     then calculate the corresponding  $APT_2^{(t)}$  according to (32a), and send  $\mathcal{C}^{(t)}$  to the
      $(t + 1)$ th iteration;
10 until  $t = Itermax$  or  $\|APT_2^{(t)} - APT_1^{(t)}\| \leq \epsilon$ ;
11 Compute  $P_s^{tr*}$  according to Proposition 3;
12 Return  $\mathcal{C}^*, \eta^*$ 

```

Then after cache decision in Algorithm 1 for given η_{t+1} , we can get

$$APT(\eta_{t+1}, C_t) \leq APT(\eta_{t+1}, C_{t+1}) \quad (38)$$

Combining (37) with (38), it holds that

$$APT(\eta_t, C_t) \leq APT(\eta_{t+1}, C_{t+1}) \quad (39)$$

This illustrates that APT value will not decrease in each iteration. The APT upper bound of cache-enabled mABHetNets is limited to a finite value, so the proposed JCSPA algorithm will converge.

V. PERFORMANCE EVALUATION

In this section, we use numerical simulation results to validate and evaluate of APT of the cache-enabled mABHetNet. Particularly, we compare APT under different scenarios.

A. Parameter Setting

Unless otherwise specified, the parameters of the simulation scenario are set as follows. The BSs and users are distributed in a square area $1000\text{m} \times 1000\text{m}$. Note that the density of the users is assumed to be sufficiently larger than that of the BS, we assume that the BS is active in the downlink. In other words, each SBS is in a backhaul association cell and has at least one associated user in its coverage. Some default simulation configurations are listed in Table II, based on 3GPP specification and literatures [15], [24], [46]–[49]. All the above settings can be changed according to different scenarios.

TABLE II: Simulation Parameters

Parameters	Physics meaning	Values
W	Total mmWave bandwidth	400 MHz
λ_s, λ_m	The density of SBS and MBS	10^{-4} BSs/m ² , 4×10^{-5} BSs/m ²
A_L, α_L	Pathloss parameters of LOS	10^{-10} , 2
A_{NL}, α_{NL}	Pathloss parameters of NLOS	10^{-14} , 4
N_0	Noise power	-90 dBm
P_s^{\max}, P_m^{\max}	Maximum power of SBS and MBS	38.2 dBm, 60 dBm
γ_0	SINR threshold	10 dB
$P_s^{\text{fc}}, P_m^{\text{fc}}$	Fixed circuit power at SBS and MBS	20 dBm, 46 dBm
ρ_s, ρ_m	Power amplifier and cooling coefficient	1, 1.5
B_s, B_m	Association biases of SBS and MBS	10, 5
β	Blockage density	2×10^{-3}
θ	Main lobe beamwidth	30°
M, m	Main lobe antenna gain, slide lobe antenna gain	10dB, -10dB
ω_{ca}	Caching power coefficient	6.25×10^{-12} W/bit
s	Size of each file	100 MB
F	The file units in the file library	1000
C_{\max}	Maximum caching capacity(file units) of SBS	800
γ_p	Zipf parameter	1.0

B. Convergence of JCSPA

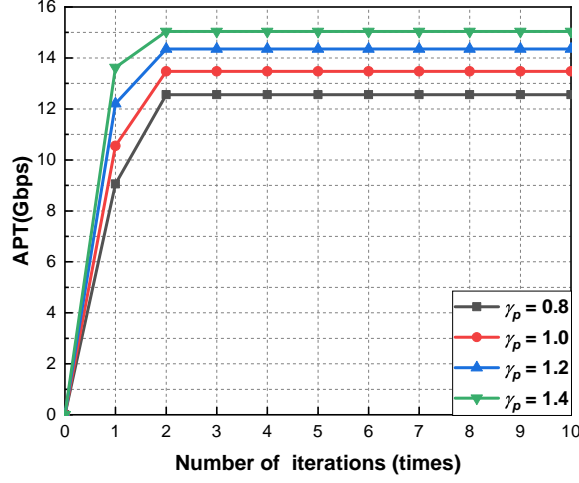


Fig. 3. Convergence performance of the proposed JCSPA algorithm in APT maximization problem.

In this subsection, simulations are carried out to validate the convergence performance and maximum APT of the proposed JCSPA algorithm for different skewnesses of caching file popularity (from 0.8 to 1.4) as Fig. 3. As expected, we can see that the joint optimization problem converges to maximum APT after approximately no more than five iterations. It can be concluded that our proposed algorithm is fast-convergent. Besides, compared to the different Zipf parameters, a higher skewness will lead to a higher APT.

C. Performance of APT under different caching capacity and spectrum partitions

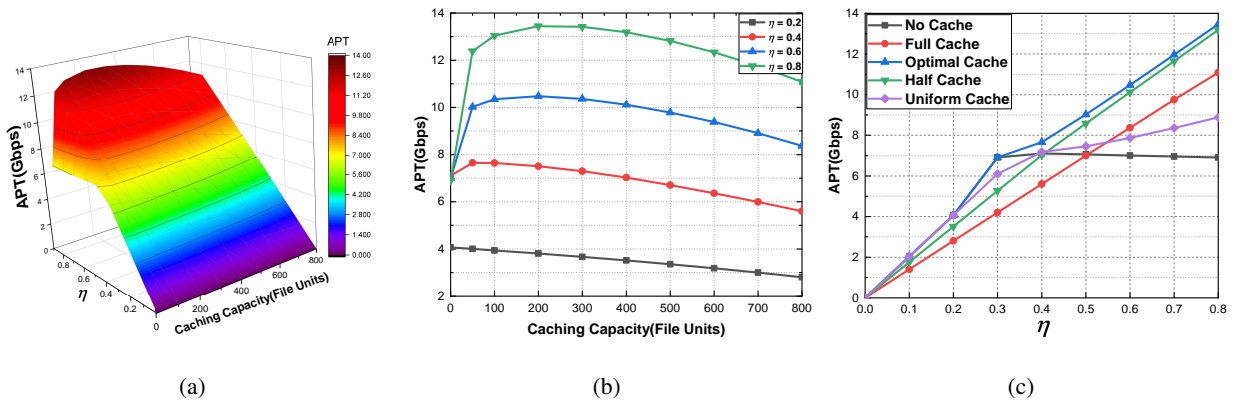


Fig. 4. APT under different caching capacity and spectrum partitions, (a) APT v.s. caching capacity & spectrum partition ratio, (b) APT v.s. caching capacity, (c) APT v.s. spectrum partition ratio.

In Fig. 4(a), the performance of APT for both the caching capacity and spectrum partition is shown. From this three-dimensional APT, both caching file capacity and spectrum partition ratio have a prominent impact on APT. APT is not monotonically increasing or decreasing with respect to these two variables.

In order to further observe their quantitative relationship, Fig. 4(b) shows the APT with respect to different caching capacity under four spectrum partition coefficients. For lower spectrum partition ratio, APT will decrease with increasing caching capacity. This is because the smaller spectrum can only satisfy the partial data transmission of the access link, and the power consumption by caching reduces the transmit power of the SBS, which further reduces the APT. While for higher spectrum partition ratio, APT will first increase with increasing caching capacity and then decrease. The reason is that as more caching files can improve the cache hit ratio of files at SBS and less files' delivery occupy backhaul resources, more files can be obtained through access link directly without backhaul link. However, APT will decrease when the caching capacity is more than about 200 file units. This is mainly because maximum power of SBS is limited and too much caching capacity consumes too much power, therefore the transmit power of SBS will be reduced, which limits the performance of APT. This gives us an insight that increasing the caching capacity does not necessarily increase the APT when the maximum power of SBS is limited.

Fig. 4(c) shows the APT of different spectrum partitions under four given caching decisions. In the case of no cache, APT will increase and then decrease with increasing spectrum partition. While for higher spectrum partition ratio, the introduction of cache at SBS increases the APT significantly. This is because caching files at SBS can transfer the spectrum from the backhaul link to the access link, which potentially improves the APT.

D. Comparison with baseline algorithms

The proposed JCSPA algorithm is compared with three basic algorithms in this subsection.

- **No cache and DSA:** This algorithm is used to optimize the spectrum partition while the SBS does not cache any files in the network [15]. This means that all files are cache-miss and the file delivery needs to go through both the access and backhaul link.
- **Optimal cache and FSA:** This algorithm aims to optimize the cache decision with given spectrum that backhaul and access link accounts for the half of the total spectrum [27]. The SBS needs to decide how many most popular files in file library to cache.

- **Full cache and DSA:** In this algorithm, the SBS uses all the caching capacity to store the C_{\max} most popular file units. Besides, the spectrum partition is based on DSA program to improve APT as much as possible.
- **Uniform cache and DSA:** This baseline algorithm is based on caching files uniformly [18] where each file is cached with identical probability and spectrum partition scheme is dynamic spectrum partition.

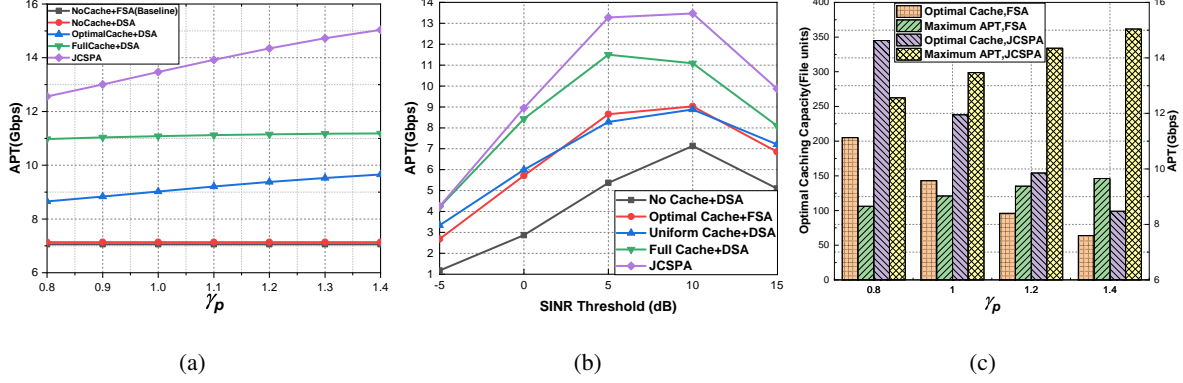


Fig. 5. Comparison of APT under different caching decision and spectrum partition algorithms, (a) APT v.s. skewness of file popularity, (b) APT v.s. SINR threshold(dB), (c) Optimal cache & APT v.s. skewness of file popularity.

In Fig. 5(a), we begin by evaluating APT in terms of different skewness of file popularity under proposed JCSPA and other three benchmark algorithms. In the cases of no cache, APT will not change with γ_p but the DSA exceeds the FSA algorithm. Besides, APT of full cache combined with DSA is better than that of optimal cache with FSA. Such result reveals the significance of the dynamic spectrum partition. In contrast, our proposed JCSPA algorithm outperforms other baseline algorithms. This illustrates the effectiveness of proposed joint optimization of cache decision and spectrum partition JCSPA algorithm.

Fig. 5(b) shows the APT with different SINR thresholds under different algorithms. Note that APT increases as SINR threshold increases when the SINR threshold is low, this is because increasing the SINR threshold γ_0 will increase the transmission rate dominates. While for larger SINR threshold, it improves the demodulation threshold of the received signal and reduces the coverage probability, so that APT will decrease with increasing the SINR threshold. Besides, the performance of JCSPA algorithm also significantly outperforms other baseline algorithms.

From Fig. 5(c) we can see that the optimal caching capacity is reduced with the increasing the

skewness while the maximum APT will increase. Comparing the two cases where $\gamma_p = 1.4$ and $\gamma_p = 0.8$, APT under JCSPA algorithm is increased by nearly 40% while the optimal caching capacity is reduced by more than 70%. In other words, only a smaller caching capacity is needed to reach the maximum APT for a higher skewness. The reason is that higher skewness helps to improve cache hit ratio, so only fewer caching file units are needed to achieve higher APT.

E. Impact of other cache parameters on APT

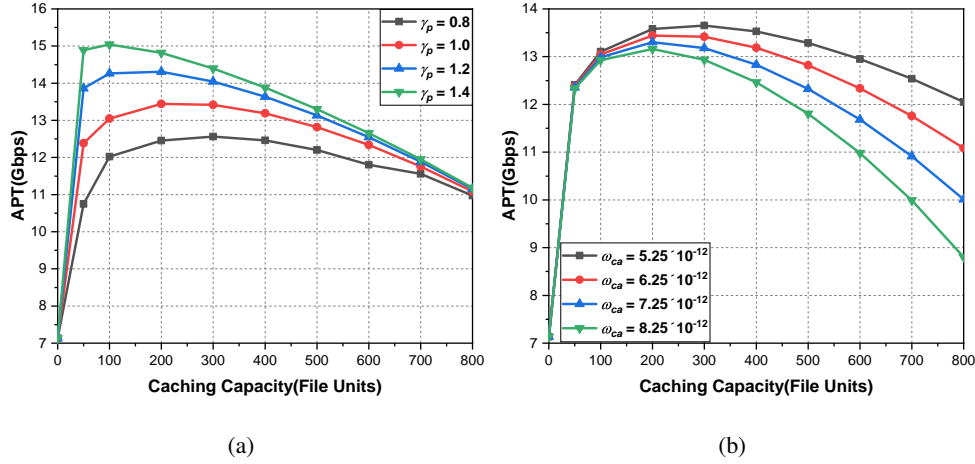


Fig. 6. Impact of cache parameters on APT, (a) APT vs. Caching capacity with different skewness γ_p , (b) APT vs. Caching capacity with different caching power coefficient ω_{ca} .

In order to obtain the impact of cache-related parameters on APT, we further give the APT of different skewness of file popularity and caching power coefficients. The skewness γ_p and caching power coefficient reflect the main characteristics of the caching. Fig. 6(a) shows the APT under different caching capacity for four skewness of caching files. It can be observed that APT first increases with caching capacity and then decreases, as well as higher skewness can lead to higher APT. This is because that higher skewness increases the cache hit ratio p_h then increases the APT. Fig. 6(b) shows the APT under different caching capacity for four caching power coefficients from 5.25×10^{-12} to 8.25×10^{-12} . When the caching capacity is small, APT is almost equal under different cache power consumption coefficients, but with the increasing of caching capacity, for the case of high cache power consumption coefficient, APT will decrease rapidly as the cache increases, while APT with lower cache power consumption coefficient decreases slowly. This is because the maximum power of SBS is limited and higher ω_{ca} will lead to more

caching power consumption for the same number of caching files, thereby reducing the transmit power and decreasing the APT. This prompts us to use storage technologies with lower caching power coefficient to improve network performance.

VI. CONCLUSION

In this paper, to cope with the “*spectrum occupancy*” problem, we make a tractable cache-enabled mABHetNet by stochastic geometry tool and investigate the impact of spectrum partition between the access link and the backhaul link as well as cache allocation on network performance. **Considering the effect of blockage and association probability**, we analyze the SINR distribution and derive the expression of APT with respect to caching capacity, spectrum partition and SINR threshold. Based on the analytical work, we optimize the cache decision and spectrum partition problem jointly to obtain the maximum APT by the proposed algorithm. Via numerical evaluations, we first evaluate the convergence of our proposed algorithm. Then we find that there exist the optimal caching capacity and spectrum partition to maximize APT, which verifies the effectiveness of our proposed algorithm. Besides, we explore the impact of some key cache-related factors on APT. The results show **up to 90% APT** gain of appropriate caching capacity and spectrum partition **compared with traditional mABHetNets**.

VII. APPENDIX

A. The proof of Lemma 1

We first consider the event that the distance between the typical user and the nearest LOS SBS (LOS based file transmission between the typical user and the SBS) is r . In fact, the event that is the joint of following two events: The first event is the nearest SBS of the typical user is located at distance r (Event 1) and the second event is the transmission path between the typical user and the serving SBS is an LOS path (Event 2). According to [50], the PDF of Event 1 with regard to r is given by $\exp(-\pi r^2 \lambda_s) \times 2\pi r \lambda_s$. The probability of Event 2 over distance r is $\mathcal{P}_L(r)$, so that we can get the PDF of the joint Event 1 and Event 2 as

$$f_{R_s}^k(r) = \mathcal{P}_k(r) \times 2\pi r \lambda_s \times \exp(-\pi r^2 \lambda_s), \quad (40)$$

where $k = \{L \text{ or } NL\}$ denotes the LOS or NLOS transmission link.

Similarly, the PDF of the distance r (between the SBS and the associated LOS MBS or NLOS MBS) is

$$f_{R_m}^k(r) = \mathcal{P}_k(r) \times 2\pi r \lambda_m \times \exp(-\pi r^2 \lambda_m). \quad (41)$$

B. The proof of Lemma 2

The typical user may be associated with the SBS tier by either LOS channel or NLOS channel. We derive the probability of the first event that the user is associated with the SBS by the wireless LoS link. Such event has other cases: the interference from the NLOS SBS and the interference from the LoS. Therefore, the probability that the user obtain the desired LOS signal from the SBS is $F_s^L(r) = p_{ln}^{ss}(r)p_{ll}^{sm}(r)p_{ln}^{sm}(r)f_{R_s}^L(r)$, where

- 1) **When the recieved power from LOS SBS is higher than that from NLOS SBS** , the user is associated with the LOS SBS and the interference is from NLOS SBS.

$$p_{ln}^{ss}(r) = \mathbb{P}[P_s^{tr} B_s G_s h_s A_L r^{-\alpha_L} \geq P_s^{tr} B_s G_s h_s A_{NL} r_s^{-\alpha_{NL}}] \quad (42)$$

$$= \mathbb{P}\left[r_s \geq \left(\frac{A_L}{A_{NL}}\right)^{\frac{-1}{\alpha_{NL}}} r^{\frac{\alpha_L}{\alpha_{NL}}}\right] = \int_0^{\left(\frac{A_L}{A_{NL}}\right)^{\frac{-1}{\alpha_{NL}}} r^{\frac{\alpha_L}{\alpha_{NL}}}} f_{R_s}(r) dr = e^{-\lambda_s \pi \left[\left(\frac{A_L}{A_{NL}}\right)^{\frac{-1}{\alpha_{NL}}} r^{\frac{\alpha_L}{\alpha_{NL}}}\right]^2}, \quad (43)$$

where the last step is based on the CDF of PPP in [50].

- 2) **Similarly, the user is associated with the LOS SBS and the interference is from LOS MBS.**

$$p_{ll}^{sm}(r) = \mathbb{P}[P_s^{tr} B_s G_s h_s A_L r^{-\alpha_L} \geq P_m^{tr} B_m G_m h_m A_L r_m^{-\alpha_L}] \quad (44)$$

$$= \mathbb{P}\left[r_m \geq \left(\frac{P_s^{tr} B_s G_s h_s}{P_m^{tr} B_m G_m h_m}\right)^{\frac{-1}{\alpha_L}} r\right] = e^{-\lambda_m \pi \left[\left(\frac{P_s^{tr} B_s G_s h_s}{P_m^{tr} B_m G_m h_m}\right)^{\frac{-1}{\alpha_L}} r\right]^2}, \quad (45)$$

- 3) **The user is associated with the LOS SBS and the interference is from NLOS MBS.**

$$p_{ln}^{sm}(r) = \mathbb{P}[P_s^{tr} B_s G_s h_s A_L r^{-\alpha_L} \geq P_m^{tr} B_m G_m h_m A_{NL} r_m^{-\alpha_{NL}}] \quad (46)$$

$$= \mathbb{P}\left[r_m \geq \left(\frac{P_s^{tr} B_s G_s h_s A_L}{P_m^{tr} B_m G_m h_m A_{NL}}\right)^{\frac{-1}{\alpha_{NL}}} r^{\frac{\alpha_L}{\alpha_{NL}}}\right] = e^{-\lambda_m \pi \left[\left(\frac{P_s^{tr} B_s G_s h_s A_L}{P_m^{tr} B_m G_m h_m A_{NL}}\right)^{\frac{-1}{\alpha_{NL}}} r^{\frac{\alpha_L}{\alpha_{NL}}}\right]^2}. \quad (47)$$

Then, the probability that the user obtain the desired NLOS signal from the SBS is

$$F_s^{NL}(r) = p_{nl}^{ss}(r)p_{nl}^{sm}(r)p_{nn}^{sm}(r)f_{R_s}^{NL}(r),$$

- 1) The user is associated with the NLoS SBS and the interference is from LOS SBS.

$$p_{nl}^{ss}(r) = \mathbb{P}[P_s^{tr} B_s G_s h_s A_{NL} r^{-\alpha_{NL}} \geq P_s^{tr} B_s G_s h_s A_L r_s^{-\alpha_L}] = e^{-\lambda_s \pi \left[\left(\frac{A_{NL}}{A_L} \right)^{\frac{-1}{\alpha_L}} r^{\frac{\alpha_{NL}}{\alpha_L}} \right]^2}. \quad (48)$$

- 2) The user is associated with the NLoS SBS and the interference is from LOS MBS.

$$p_{nl}^{sm}(r) = \mathbb{P}[P_s^{tr} B_s G_s h_s A_{NL} r^{-\alpha_{NL}} \geq P_m^{tr} B_m G_m h_m A_L r_m^{-\alpha_L}] = e^{-\lambda_m \pi \left[\left(\frac{P_s^{tr} B_s G_s h_s A_{NL}}{P_m^{tr} B_m G_m h_m A_L} \right)^{\frac{-1}{\alpha_L}} r^{\frac{\alpha_{NL}}{\alpha_L}} \right]^2}. \quad (49)$$

- 3) The user is associated with the NLoS SBS and the interference is from NLoS MBS.

$$p_{nn}^{sm}(r) = \mathbb{P}[P_s^{tr} B_s G_s h_s A_{NL} r^{-\alpha_{NL}} \geq P_m^{tr} B_m G_m h_m A_{NL} r_m^{-\alpha_{NL}}] = e^{-\lambda_m \pi \left[\left(\frac{P_s^{tr} B_s G_s h_s}{P_m^{tr} B_m G_m h_m} \right)^{\frac{-1}{\alpha_{NL}}} r \right]^2}. \quad (50)$$

Then, the probability that the user obtain the desired LoS signal from the MBS is $F_m^L(r) = p_{1n}^{mm}(r) p_{ll}^{ms}(r) p_{ln}^{sm}(r) f_{R_m}^L(r)$ where

- 1) The user is associated with the LoS MBS and the interference is from NLoS MBS.

$$p_{ln}^{mm}(r) = \mathbb{P}[P_m^{tr} B_m G_m h_m A_L r^{-\alpha_L} \geq P_m^{tr} B_m G_m h_m A_{NL} r_m^{-\alpha_{NL}}] = e^{-\lambda_m \pi \left[\left(\frac{A_L}{A_{NL}} \right)^{\frac{-1}{\alpha_{NL}}} r^{\frac{\alpha_L}{\alpha_{NL}}} \right]^2} \quad (51)$$

- 2) The user is associated with the LoS MBS and the interference is from LoS SBS.

$$p_{ll}^{ms}(r) = \mathbb{P}[P_m^{tr} B_m G_m h_m A_L r^{-\alpha_L} \geq P_s^{tr} B_s G_s h_s A_L r_s^{-\alpha_L}] = e^{-\lambda_s \pi \left[\left(\frac{P_m^{tr} B_m h_m}{P_s^{tr} B_s h_s} \right)^{\frac{-1}{\alpha_L}} r \right]^2} \quad (52)$$

- 3) The user is associated with the LoS MBS and the interference is from NLoS SBS.

$$p_{ln}^{sm}(r) = \mathbb{P}[P_m^{tr} B_m G_m h_m A_L r^{-\alpha_L} \geq P_s^{tr} B_s G_s h_s A_{NL} r_s^{-\alpha_{NL}}] = e^{-\lambda_s \pi \left[\left(\frac{P_m^{tr} B_m G_m h_m A_L}{P_s^{tr} B_s G_s h_s A_{NL}} \right)^{\frac{-1}{\alpha_{NL}}} r^{\frac{\alpha_L}{\alpha_{NL}}} \right]^2} \quad (53)$$

Following the same logic, the probability that the user obtain the desired NLoS signal from the MBS is $F_m^{NL}(r) = p_{nl}^{mm}(r) p_{nl}^{ms}(r) p_{nn}^{sm}(r) f_{R_m}^{NL}(r)$

The probability that SBS obtains the desired LOS or NLOS signal from MBS is

$$F_{bh}^L(r) = p_{ln}^{bh}(r) f_{R_{bh}}^L(r),$$

where the probability that the SBS is associated with the LOS MBS and the interference is from NLOS MBS is

$$p_{ln}^{bh}(r) = \mathbb{P}[P_m^{tr} B_m \mathbf{G}_m h_m A_L r^{-\alpha_L} \geq P_m^{tr} B_m \mathbf{G}_m h_m A_{NL} r_{bh}^{-\alpha_{NL}}] = e^{-\lambda_m \pi \left[\left(\frac{A_L}{A_{NL}} \right)^{\frac{-1}{\alpha_{NL}}} r^{\frac{\alpha_L}{\alpha_{NL}}} \right]^2}.$$

Similarly, $F_{bh}^{NL}(r) = p_{nl}^{bh}(r) f_{R_{bh}}^{NL}(r)$.

C. Proof of Proposition 1

Then we first focus on the SINR distribution of a user covered by SBS:

$$P_s^{cov}(\gamma) = P_{s,L}^{cov}(\gamma) + P_{s,NL}^{cov}(\gamma), \quad (54)$$

where the SINR distribution of a user covered by LOS/NLOS SBS:

$$P_{s,k}^{cov}(\gamma) = \mathbb{E}_r [\mathbb{P} [\text{SINR}_s^k(r) > \gamma]] = \int_0^\infty \mathbb{P} [\text{SINR}_s^k(r) > \gamma] F_s^k(r) dr, \quad (55)$$

where $k = \{L \text{ or } NL\}$ denotes the LOS or NLOS transmission link,

γ is the threshold for successful demodulation and decoding at the receiver. $\mathbb{P} [\text{SINR}_s^L(r) > \gamma]$ means the probability of the event that the SINR of the user covered by SBS is over γ via the LOS path at distance r :

$$\begin{aligned} \mathbb{P} [\text{SINR}_s^k(r) > \gamma] &= \mathbb{P} \left[\frac{P_s^{tr} B_s \mathbf{G}_s h_s A_k r^{-\alpha_k}}{I_s + I_m + N_0} > \gamma \right] \\ &= \mathbb{P} \left[h_s > \frac{\gamma (I_s + I_m + N_0)}{P_s^{tr} B_s \mathbf{G}_s A_k r^{-\alpha_k}} \right] \stackrel{(a)}{=} \exp \left(\frac{-\gamma N_0}{P_s^{tr} B_s \mathbf{G}_s A_k r^{-\alpha_k}} \right) \mathcal{L}_{I_{s,m}}^k(\gamma r^{\alpha_k}), \end{aligned} \quad (56)$$

where (a) follows from small fading $h \sim \exp(1)$. Here the Rayleigh fading is considered. $\mathcal{L}_{I_{s,m}}$ is the Laplace transform of the cumulative interference from the SBS tier and the MBS tier.

$$\mathcal{L}_{I_{s,m}}^L(\gamma r^{\alpha_L})$$

$$\begin{aligned} &\stackrel{(b)}{=} \prod_{G_i} \exp \left(-2\pi \lambda_s p_{G_i} \int_r^\infty \left(\frac{\mathcal{P}_L(u) u}{1 + \frac{P_s^{tr} B_s \mathbf{G}_s A_L r^{-\alpha_L}}{\gamma P_s^{tr} B_s \mathbf{G}_i A_L u^{-\alpha_L}}} du \right) \right) \prod_{G_i} \exp \left(-2\pi \lambda_s p_{G_i} \int_{\left(\frac{A_L}{A_{NL}} \right)^{\frac{-1}{\alpha_{NL}}} r^{\frac{\alpha_L}{\alpha_{NL}}}}^\infty \left(\frac{\mathcal{P}_{NL}(u) u}{1 + \frac{P_s^{tr} B_s \mathbf{G}_s A_L r^{-\alpha_L}}{\gamma P_s^{tr} B_s \mathbf{G}_i A_{NL} u^{-\alpha_{NL}}}} du \right) \right) \\ &\times \prod_{G_l} \exp \left(-2\pi \lambda_m p_{G_l} \int_{(d_1)^{\frac{-1}{\alpha_L}} r}^\infty \left(\frac{\mathcal{P}_L(u) u}{1 + \frac{P_s^{tr} B_s \mathbf{G}_s A_L r^{-\alpha_L}}{\gamma P_m^{tr} B_m \mathbf{G}_l A_L u^{-\alpha_L}}} du \right) \right) \prod_{G_l} \exp \left(-2\pi \lambda_m p_{G_l} \int_{(d_2)^{\frac{-1}{\alpha_{NL}}} r^{\frac{\alpha_L}{\alpha_{NL}}}}^\infty \left(\frac{\mathcal{P}_{NL}(u) u}{1 + \frac{P_s^{tr} B_s \mathbf{G}_s A_L r^{-\alpha_L}}{\gamma P_m^{tr} B_m \mathbf{G}_l A_{NL} u^{-\alpha_{NL}}}} du \right) \right) \end{aligned}$$

where p_{G_i} and p_{G_l} is the probability of the antenna gain taking corresponding value from SBS interference tier and MBS interference tier. Step (b) is based on the PGFL of PPP [50]. $d_1 = \frac{P_s^{tr} B_s}{P_m^{tr} B_m}$ and $d_2 = \frac{P_s^{tr} B_s A_L}{P_m^{tr} B_m A_{NL}}$. Following the same logic, other Laplace transforms of cumulative interference $\mathcal{L}_{I_s}^{NL}(\gamma r^{\alpha_{NL}})$, $\mathcal{L}_{I_{bh}}^L(\gamma r^{\alpha_L})$, $\mathcal{L}_{I_{bh}}^{NL}(\gamma r^{\alpha_{NL}})$ can also be obtained.

Similarly, the SINR distribution of SBS is covered by MBS:

$$P_{bh}^{cov}(\gamma) = P_{bh,L}^{cov}(\gamma) + P_{bh,NL}^{cov}(\gamma) \quad (57)$$

$$\begin{aligned} &= \mathbb{E}_r [\mathbb{P} [\text{SINR}_{bh}^L(r) > \gamma]] + \mathbb{E}_r [\mathbb{P} [\text{SINR}_{bh}^{NL}(r) > \gamma]] \\ &= \int_0^\infty \mathbb{P} [\text{SINR}_{bh}^L(r) > \gamma] F_{bh}^L(r) dr + \int_0^\infty \mathbb{P} [\text{SINR}_{bh}^{NL}(r) > \gamma] F_{bh}^{NL}(r) dr, \end{aligned}$$

where $\mathbb{P} [\text{SINR}_{bh}^L(r) > \gamma] = \exp\left(\frac{-\gamma N_0}{P_m^{tr} B_m A_L r^{-\alpha_L}}\right) \mathcal{L}_{I_{bh}}^L(\gamma r^{\alpha_L})$ and $\mathbb{P} [\text{SINR}_{bh}^{NL}(r) > \gamma]$
 $= \exp\left(\frac{-\gamma N_0}{P_m^{tr} B_m A_{NL} r^{-\alpha_{NL}}}\right) \mathcal{L}_{I_{bh}}^{NL}(\gamma r^{\alpha_{NL}}).$

D. Proof of Proposition 2

In noise-limited scenario, the interference is close to zero, so the SINR distribution can be reduced to

$$P_k^{cov}(\gamma) = \mathbb{P}\left[\frac{P_k g B_k G_k A r^{-\alpha}}{\sigma^2} > \gamma\right] = \mathbb{P}\left[\frac{r^\alpha}{A g} < \frac{P_k B_k G_k}{\sigma^2 \gamma}\right]$$

where $A \in \{A_L, A_{NL}\}$, $\alpha \in \{\alpha_L, \alpha_{NL}\}$. Considering the effect of blockage, the intensity function of process $\Lambda = \{r^\alpha\} = \{\phi\}$ is calculated as

$$\Lambda(\phi) = \int_0^{(A_L \phi)^{\frac{1}{\alpha_L}}} 2\pi \lambda_k u e^{-\beta u} du + \int_0^{(A_{NL} \phi)^{\frac{1}{\alpha_{NL}}}} 2\pi \lambda_k u (1 - e^{-\beta u}) du \quad (58)$$

where $k \in \{m, s\}$ denotes the MBS tier or SBS tier. Then, the density function is

$$\lambda(\phi) = \frac{d\Lambda(\phi)}{d\phi} = \frac{2\pi \lambda_k A_{NL}}{\alpha_{NL}} (A_{NL} \phi)^{\frac{2}{\alpha_{NL}}-1} + \frac{2\pi \lambda_k (A_L \phi)^{\frac{2}{\alpha_L}-1}}{\alpha_L e^{\beta (A_L \phi)^{\frac{1}{\alpha_L}}}} - \frac{2\pi \lambda_k (A_{NL} \phi)^{\frac{2}{\alpha_{NL}}-1}}{\alpha_{NL} e^{\beta (A_{NL} \phi)^{\frac{1}{\alpha_{NL}}}}} \quad (59)$$

Then, the joint distribution fuction and probability density function of $\{\phi, g\}$ can be given as

$$\mathbb{P}\left[\frac{\phi}{g} \leq \xi\right] = \mathbb{P}\left[g \geq \frac{\phi}{\xi}\right] = 1 - F_g\left(\frac{\phi}{\xi}\right) \quad (60)$$

$$\rho(\phi, \xi) = \frac{d(1 - F_g(\frac{\phi}{\xi}))}{d\xi} = \frac{\phi}{\xi^2} f_g\left(\frac{\phi}{\xi}\right) \stackrel{(a)}{=} \frac{\phi}{\xi^2} e^{-\frac{\phi}{\xi}} \quad (61)$$

where step (a) is based on the Rayleigh fading channel with exponential distribution ($h \sim \exp(1)$). Based on the displacement theorem, the density function of process $\Xi = \{\frac{\phi}{g}\} = \{\xi\}$ can be obtained as

$$\begin{aligned} \lambda_\Xi(\xi) &= \int_0^\infty \lambda(\phi) \rho(\phi, \xi) d\phi \\ &= \int_0^\infty \left(\frac{2\pi \lambda_k A_{NL}}{\alpha_{NL}} (A_{NL} \phi)^{\frac{2}{\alpha_{NL}}-1} + \frac{2\pi \lambda_k (A_L \phi)^{\frac{2}{\alpha_L}-1}}{\alpha_L e^{\beta (A_L \phi)^{\frac{1}{\alpha_L}}}} - \frac{2\pi \lambda_k (A_{NL} \phi)^{\frac{2}{\alpha_{NL}}-1}}{\alpha_{NL} e^{\beta (A_{NL} \phi)^{\frac{1}{\alpha_{NL}}}}} \right) \frac{\phi}{\xi^2} e^{-\frac{\phi}{\xi}} d\phi \\ &= \frac{2\pi \lambda_k A_{NL}^{\frac{2}{\alpha_{NL}}}}{\alpha_{NL}} \xi^{\frac{2}{\alpha_{NL}}-1} \Gamma\left(\frac{2}{\alpha_{NL}} + 1\right) + \frac{2\pi \lambda_k}{\xi^2} (H_L - H_{NL}) \end{aligned} \quad (62)$$

where $H_i = \frac{A_i^{\frac{2}{\alpha_i}-1}}{\alpha_i} \int_0^\infty \phi^{\frac{2}{\alpha_i}} \exp(-\beta(A_i\phi)^{\frac{1}{\alpha_i}} - \frac{\phi}{\xi}) d\phi$, $i \in \{L, NL\}$. Now, based on the complementary void function of PPP, the CDF of ξ is given by

$$\begin{aligned} F_\Xi(\xi_0) &= \mathbb{P}[\xi < \xi_0] = 1 - \mathbb{P}[\Xi(\xi_0) = 0] = 1 - \exp(-\int_0^{\xi_0} \lambda_\Xi(\xi) d\xi) \\ &= 1 - \exp(-\pi \lambda_k A_{NL}^{\frac{2}{\alpha_{NL}}} \Gamma(\frac{1}{\alpha_{NL}} + 1) \xi_0^{\frac{2}{\alpha_{NL}}} - 2\pi \lambda_k Y(\xi_0)) \end{aligned} \quad (63)$$

where $Y(\xi_0) = \int_0^{\xi_0} \frac{A_L^{\frac{2}{\alpha_L}-1}}{\alpha_L \xi^2} \int_0^\infty \phi^{\frac{2}{\alpha_L}} \exp(-\beta\phi^{\frac{1}{\alpha_L}} - \frac{\phi}{\xi}) d\phi d\xi - \int_0^{\xi_0} \frac{A_{NL}^{\frac{2}{\alpha_{NL}}-1}}{\alpha_{NL} \xi^2} \int_0^\infty \phi^{\frac{2}{\alpha_{NL}}} \exp(-\beta\phi^{\frac{1}{\alpha_{NL}}} - \frac{\phi}{\xi}) d\phi d\xi$. Then we can obtain that

$$\begin{aligned} P_k^{cov}(\gamma) &= \mathbb{P}[\frac{r^\alpha}{g} < \frac{P_k B_k G_k}{\sigma^2 \gamma}] = F_\Xi(\frac{P_k B_k G_k}{\sigma^2 \gamma}) \\ &= 1 - \exp\left(-\pi \lambda_k A_{NL}^{\frac{2}{\alpha_{NL}}} \Gamma\left(\frac{1}{\alpha_{NL}} + 1\right) \left(\frac{P_k B_k G_k}{\sigma^2 \gamma}\right)^{\frac{2}{\alpha_{NL}}} - 2\pi \lambda_k Y\left(\frac{P_k B_k G_k}{\sigma^2 \gamma}\right)\right) \end{aligned} \quad (64)$$

REFERENCES

- [1] C. Zhang, H. Wu, H. Lu and J. Liu, "Throughput Analysis in Cache-enabled Millimeter Wave HetNets with Access and Backhaul Integration," in *Proc. Wireless Commun. Netw. Conf.(WCNC)*, May. 2020, pp. 1-6.
- [2] Cisco, "Cisco Visual Networking Index: Global Mobile Data Traffic Forecast Update, 2017–2022," *White Paper*, Feb. 2019.
- [3] C. Madapatha et al., "On Integrated Access and Backhaul Networks: Current Status and Potentials," *IEEE Open J. Commun. Soc.*, vol. 1, pp. 1374–1389, Sep. 2020.
- [4] C. Dehos, J. L. González, A. De Domenico, D. Kténas, and L. Dussot, "Millimeter-wave Access and Backhauling: The Solution to the Exponential Data Traffic Increase in 5G Mobile Communications Systems?" *IEEE Commun. Mag.*, vol. 52, no. 9, pp. 88–95, Sept. 2014.
- [5] R. Taori and A. Sridharan, "Point-to-Multipoint in-band Mmwave Backhaul for 5G Networks," *IEEE Commun. Mag.*, vol. 53, no. 1, pp. 195–201, Jan. 2015.
- [6] R. J. Weiler et al., "Enabling 5G Backhaul and Access with Millimeter-waves," in *Proc. IEEE EuCNC* 2014, Bologna, 2014, pp. 1-5.
- [7] NR; Study on Integrated Access and Backhaul, document 3GPP TR 38.874, 2017.
- [8] *Service Requirements for the 5G System*, document 3GPP TS 22.261, Jan. 2018.
- [9] A. AlAmmouri, J. G. Andrews and F. Baccelli, "A Unified Asymptotic Analysis of Area Spectral Efficiency in Ultradense Cellular Networks," *IEEE Trans. Inf. Theory*, vol. 65, no. 2, pp. 1236–1248, Feb. 2019.
- [10] X. Zhang and J. G. Andrews, "Downlink Cellular Network Analysis With Multi-Slope Path Loss Models," *IEEE Trans. Commun.*, vol. 63, no. 5, pp. 1881–1894, May. 2015.
- [11] I. Atzeni, J. Arnau and M. Kountouris, "Downlink Cellular Network Analysis With LOS/NLOS Propagation and Elevated Base Stations," *IEEE Trans. Wireless Commun.*, vol. 17, no. 1, pp. 142–156, Jan. 2018.
- [12] W. Yi, Y. Liu and A. Nallanathan, "Modeling and Analysis of D2D Millimeter-Wave Networks With Poisson Cluster Processes," *IEEE Trans. Commun.*, vol. 65, no. 12, pp. 5574–5588, Dec. 2017.

- [13] C. Saha and H. S. Dhillon, "Millimeter Wave Integrated Access and Backhaul in 5G: Performance Analysis and Design Insights," *IEEE J. Sel. Areas Commun.*, vol. 37, no. 12, pp. 2669-2684, Dec. 2019.
- [14] S. Hur, T. Kim, D. J. Love, J. V. Krogmeier, T. A. Thomas and A. Ghosh, "Millimeter Wave Beamforming for Wireless Backhaul and Access in Small Cell Networks," *IEEE Trans. Commun.*, vol. 61, no. 10, pp. 4391-4403, Oct. 2013.
- [15] Z. Shi, Y. Wang, L. Huang and T. Wang, "Dynamic Resource Allocation in MmWave Unified Access and Backhaul Network," *Proc. PIMRC*, Hong Kong, 2015, pp. 2260-2264.
- [16] C. Saha, M. Afshang and H. S. Dhillon, "Bandwidth Partitioning and Downlink Analysis in Millimeter Wave Integrated Access and Backhaul for 5G," *IEEE Trans. Wireless Commun.*, vol. 17, no. 12, pp. 8195-8210, Dec. 2018.
- [17] M. Diamanti, P. Charatsaris, E. E. Tsiropoulou and S. Papavassiliou, "The Prospect of Reconfigurable Intelligent Surfaces in Integrated Access and Backhaul Networks," *IEEE Trans. on Green Commun. Netw.*, Early access, Nov. 2021, doi: 10.1109/TGCN.2021.3126784.
- [18] D. Liu, B. Chen, C. Yang and A. F. Molisch, "Caching at the Wireless Edge: Design Aspects, Challenges, and Future Directions," *IEEE Commun. Mag.*, vol. 54, no. 9, pp. 22-28, 2016.
- [19] M. Tao, E. Chen, H. Zhou and W. Yu, "Content-centric Sparse Multicast Beamforming for Cache-enabled Cloud RAN," *IEEE Trans. Wireless Commun.*, vol. 15, no. 9, pp. 6118-6131, Sept. 2016.
- [20] X. Xu and M. Tao, "Modeling, Analysis, and Optimization of Coded Caching in Small-cell Networks," *IEEE Trans. Commun.*, vol. 65, no. 8, pp. 3415-3428, Aug. 2017.
- [21] C. Fan, T. Zhang, Y. Liu and Z. Zeng, "Cache-Enabled HetNets With Limited Backhaul: A Stochastic Geometry Model," *IEEE Trans. Commun.*, vol. 68, no. 11, pp. 7007-7022, Nov. 2020.
- [22] Y. Chiang and W. Liao, "ENCORE: An Energy-aware Multicell Cooperation in Heterogeneous Networks with Content Caching," *Proc. IEEE INFOCOM*, San Francisco, CA, 2016, pp. 1-9.
- [23] G. Auer et al., "How much energy is needed to run a wireless network?," *IEEE Trans. Wireless Commun.*, vol. 18, no. 5, pp. 40-49, Oct. 2011.
- [24] D. Liu and C. Yang, "Energy Efficiency of Downlink Networks With Caching at Base Stations," *IEEE J. Sel. Areas Commun.*, vol. 34, no. 4, pp. 907-922, Apr. 2016.
- [25] Z. Gu, H. Lu and Z. Zhu, "On Throughput Optimization and Bound Analysis in Cache-Enabled Fiber-Wireless Networks," *IEEE Trans. Veh. Technol.*, vol. 69, no. 8, pp. 9068-9082, Aug. 2020.
- [26] F. Gabry, V. Bioglio and I. Land, "On Energy-Efficient Edge Caching in Heterogeneous Networks," *IEEE J. Sel. Areas Commun.*, vol. 34, no. 12, pp. 3288-3298, Dec. 2016.
- [27] B. Dai, Y. Liu and W. Yu, "Optimized Base-Station Cache Allocation for Cloud Radio Access Network With Multicast Backhaul," *IEEE J. Sel. Areas Commun.*, vol. 36, no. 8, pp. 1737-1750, Aug. 2018.
- [28] H. Elsayy, E. Hossain, and M. Haenggi, "Stochastic geometry for modeling, analysis, and design of multi-tier and cognitive cellular wireless networks: A survey," *IEEE Commun. Surveys Tuts.*, vol. 15, no. 3, pp. 996-1019, Jun. 2013.
- [29] J. Llorca et al., "Dynamic In-network Caching for Energy Efficient Content Delivery," in *Proc. IEEE INFOCOM*, 2013, pp. 245-249.
- [30] K. Shanmugam, N. Golrezaei, A. G. Dimakis, A. F. Molisch and G. Caire, "FemtoCaching: Wireless Content Delivery Through Distributed Caching Helpers," *IEEE Trans. Inf. Theory*, vol. 59, no. 12, pp. 8402-8413, Dec. 2013.
- [31] P. Gill, M. Arlitt, Z. Li, and A. Mahanti, "YouTube Traffic Characterization: A View from the Edge," in *Proc. ACM IMC*, San Diego, CA, Oct. 2007.
- [32] L. Wang, K. Wong, S. Lambotharan, A. Nallanathan and M. ElKashlan, "Edge Caching in Dense Heterogeneous Cellular Networks With Massive MIMO-Aided Self-Backhaul," *IEEE Trans. Wireless Commun.*, vol. 17, no. 9, pp. 6360-6372, Sep. 2018.

- [33] L. Breslau, P. Cao, L. Fan, G. Phillips, and S. Shenker, "Web Caching and Zipf-like Distributions: Evidence and Implications," in *Proc. IEEE INFOCOM*, 1999, pp. 126–134.
- [34] M. Cha, P. Rodriguez, J. Crowcroft, S. Moon, and X. Amatriain, "Watching Television over An IP Network," in *Proc. ACM SIGCOMM IMC*, 2008, pp. 126–134.
- [35] X. Zhang, T. Lv, W. Ni, J. M. Cioffi, N. C. Beaulieu and Y. J. Guo, "Energy-Efficient Caching for Scalable Videos in Heterogeneous Networks," *IEEE J. Sel. Areas Commun.*, vol. 36, no. 8, pp. 1802-1815, Aug. 2018.
- [36] F. Gabry, V. Bioglio and I. Land, "On Energy-Efficient Edge Caching in Heterogeneous Networks," *IEEE J. Sel. Areas Commun.*, vol. 34, no. 12, pp. 3288-3298, Dec. 2016.
- [37] J. Llorca, A. M. Tulino, M. Varvello, J. Esteban and D. Perino, "Energy Efficient Dynamic Content Distribution," *IEEE J. Sel. Areas Commun.*, v, vol. 33, no. 12, pp. 2826-2836, Dec. 2015.
- [38] G. Quer, I. Pappalardo, B. D. Rao and M. Zorzi, "Proactive Caching Strategies in Heterogeneous Networks With Deviceto-Device Communications," *IEEE Trans. Wireless Commun.*, vol. 17, no. 8, pp. 5270-5281, Aug. 2018.
- [39] T. Bai, R. Vaze, and R. Heath, "Analysis of blockage effects on urban cellular networks," *IEEE Trans. Wireless Commun.*, vol. 13, no. 9, pp. 5070–5083, Sep. 2014.
- [40] S. Singh, M. Kulkarni, A. Ghosh, and J. Andrews, "Tractable model for rate in self-backhauled millimeter wave cellular networks," *IEEE J. Sel. Areas Commun.*, vol. 33, no. 10, pp. 2196–2211, Oct. 2015.
- [41] Y. Ye, S. Huang, M. Xiao, Z. Ma and M. Skoglund, "Cache-Enabled Millimeter Wave Cellular Networks With Clusters," *IEEE Trans. Commun.*, vol. 68, no. 12, pp. 7732-7745, Dec. 2020.
- [42] A. K. Gupta, J. G. Andrews and R. W. Heath, "On the Feasibility of Sharing Spectrum Licenses in mmWave Cellular Systems," *IEEE Trans. Commun.*, vol. 64, no. 9, pp. 3981-3995, Sept. 2016.
- [43] S. Singh, M. N. Kulkarni, A. Ghosh, and J. G. Andrews, "Tractable Model for Rate in Self-backhauled Millimeter Wave Cellular Networks," *IEEE J. Sel. Areas Commun.*, vol. 33, no. 10, pp. 2196–2211, Oct. 2015.
- [44] J. G. Andrews, T. Bai, M. N. Kulkarni, A. Alkhateeb, A. K. Gupta, and R. W. Heath, Jr., "Modeling and Analyzing Millimeter Wave Cellular Systems," *IEEE Trans. Commun.*, vol. 65, no. 1, pp. 403–430, Jan. 2017.
- [45] E. Turgut and M. C. Gursoy, "Coverage in Heterogeneous Downlink Millimeter Wave Cellular Networks," *IEEE Trans. Commun.*, vol. 65, no. 10, pp. 4463-4477, Oct. 2017.
- [46] 3GPP TR 36.942 V12.0.0, "Radio Frequency (RF) System Scenarios (Release 12)," Sep. 2010.
- [47] M. Ding, P. Wang, D. López-Pérez, G. Mao and Z. Lin, "Performance Impact of LoS and NLoS Transmissions in Dense Cellular Networks," *IEEE Trans. Wireless Commun.*, vol. 15, no. 3, pp. 2365-2380, Mar. 2016.
- [48] M. Peng, K. Zhang, J. Jiang, J. Wang and W. Wang, "Energy-Efficient Resource Assignment and Power Allocation in Heterogeneous Cloud Radio Access Networks," *IEEE Trans. Veh. Technol.*, vol. 64, no. 11, pp. 5275-5287, Nov. 2015.
- [49] C. Liu and K. L. Fong, "Fundamentals of the Downlink Green Coverage and Energy Efficiency in Heterogeneous Networks," *IEEE J. Sel. Areas Commun.*, vol. 34, no. 12, pp. 3271-3287, Dec. 2016.
- [50] J. G. Andrews, F. Baccelli, and R. K. Ganti, "A Tractable Approach to Coverage and Rate in Cellular Networks," *IEEE Trans. Commun.*, vol. 59, no. 11, pp. 3122–3134, 2011.
- [51] D. P. Bertsekas. *Nonlinear Programming*, 2nd ed. Belmont, MA, USA: Athena Scientific, 1999.
- [52] P. Tseng, "Convergence of a block coordinate descent method for nondifferentiable minimization," *J. Optim. Theory Appl.*, vol. 109, no. 3, pp. 475–494, Jun. 2001.